NTNU – Trondheim
Norwegian University of
Science and Technology

Evaluation of Rheology and Pressure Losses for Oil-based Drilling Fluids in a Simulated Drilling Process

Dias Viktorovitsj Assembayev

Petroleum Geoscience and Engineering
Submission date: June 2015
Supervisor: Pål Skalle, IPT

Norwegian University of Science and Technology
Department of Petroleum Engineering and Applied Geophysics

Abstract

The advancements in the field of hydraulics have indicated that eccentricity in the well greatly reduces the pressure losses. This knowledge has been readily adopted in the industry practice, but the theoretical approximations of the pressure losses regarding the eccentricity have not been fully modified. The existing approximations are based on the older solutions from the concentric annulus case and suggest use of correction factors. The flow loop experimental rig of SINTEF Petroleum Research has allowed conducting experiments on eccentric annulus, allowing us to evaluate and verify the theoretical estimation method that was derived, and it has proved to give good predictions of pressure drop in eccentric annulus.

Herschel-Bulkley rheology model was found to be the model that provides the best mathematical description of the rheology of the tested oil-based fluids for the pressure loss calculations, among several other models. However, during the comparison of the experimental data with the theoretical predictions and subsequent evaluation of these some questions were raised about the quality of the rheological measurements and the methodology used for performing these. Additional experiments were conducted with both Fann 35 viscometer and Anton Paar Physica rheometer in order to find out how pre-treatment of samples and other relevant measuring factors can affect the quality of the measurements. The result of this work has provided both quantification of the effects of these factors and suggestions for improvement of the measurement methodology, and the findings are submitted and accepted in a paper for the Nordic Rheology Society.

Sammendrag

Fremskritt innen feltet for hydraulikk har vist at borestrengeksentrisitet i brønn fører til trykktapsreduksjon i ringrommet. Denne kunnskapen ble fort akseptert i industripraksisen, men de teoretiske tilnærmingene for eksentrisitet har ikke vært fullt utviklet. Eksisterende tilnærminger er basert på eldre løsninger for konsentriske ringrom med bruk av korreksjonsfaktorer. Testriggen til SINTEF Petroleum Research i Trondheim har gjort det mulig å gjennomføre eksperimenter på eksentrisk ringrom, noe som har gitt oss muligheten til å evaluere og verifisere den teoretiske tilnærmingen som ble utledet. Denne tilnærmingen har vist seg å gi gode estimeringer av trykktap i eksentrisk ringrom.

Herschel-Bulkley modellen har vist seg å gi den beste matematiske beskrivelsen av reologien til de oljebaserte borevæskene som var brukt for trykktapsberegninger, blant alle de tilgjengelige modellene som vanligvis brukes i dette studiefeltet. Imidlertid har det blitt stilt spørsmål til kvaliteten av de reologiske målingene og metodene som var brukt til å utføre disse når man sammenlignet de eksperimentelle data med de teoretiske estimeringene og prøvd å evaluere disse. Ytterligere eksperimenter ble utført med både Fann 35 viskosimeteret og Anton Paar Physica reometeret for å finne ut hvordan forbehandling av prøver og noen andre relevante faktorer påvirker kvaliteten av målingene. Dette arbeidet har resultert i både kvantifisering av virkningene til disse og forslag til forbedring av målemetodikken, og funnene ble presentert i en artikkel og akseptert av Nordic Rheology Society.

Acknowledgement

First of all I would like to thank my supervisor Prof. Pål Skalle at NTNU and co-supervisor Jan David Ytrehus at SINTEF Petroleum Research for their guidance and helpful feedback throughout the entire project and for their help with defining the scope of this thesis.

I would like to thank PhD candidate Benjamin Werner, who has been both a good friend and a resourceful colleague in the lab during the entire semester.

A special thanks goes to Velaug Myrseth Oltedal at SINTEF Petroleum Research, who at some points has been both a supervisor and a close friend and who opened the door into the research world for me. She has been the source of inspiration and guidance for a considerable part of this thesis work.

A big thanks goes to Bjørnar Lund at SINTEF Petroleum Research, whose help has been essential in the study of pressure drops and derivation of the corresponding equations. Thanks for all your helpful feedbacks and for always being ready to help.

I would as well like to thank Knud Richard Gyland at Schlumberger for our interesting conversations on the related topic, Ali Taghipour at SINTEF Petroleum Research for always being available and ready to share his vast knowledge on the experimental rig set-up, PhD candidate Sneha Sayindla for her help and assistance with the relevant data and Roger Overå at NTNU for guidance and help with the laboratory equipment.

Trondheim, June 2015

Dias Assembayev

Table of Contents

1. Introduction

One of the main challenges in oil well drilling is to maintain mechanical well stability by keeping hydraulics under control. The reservoirs are getting ever deeper and more difficult to access, making the pressure windows even narrower. Predicting the pressure losses correctly in the well is of vital importance for designing the right drilling fluids and maintaining the well stable. The advancements in the field knowledge have indicated that eccentricity in the well greatly reduces the pressure losses. Silva and Shah (2000) claimed that the friction pressure losses in fully eccentric annulus were found to be on average 18 to 40 % lower than in concentric annulus, and that these losses were independent of the fluid type and the flow regime. Also Kelessidis et al. (2011) reported that a 100 % eccentric annulus presents pressure loss data that range from 55 % to 70 % of the concentric case.

A great share of the theoretical knowledge on pressure losses is based on the traditional case of concentric annulus. Consequently, the existing solutions are mainly adapted to it. Several works have presented approximations of pressure drop estimation in eccentric annuli. But also these are not completely innovative solutions, because they are based on previous existing solutions for concentric case and take in use correction factors. One example of lack of modified equations was given by Kelessidis et al. (2011), who reported that there is no consensus among the research community on how one can define a non-ambiguous Reynolds number for an eccentric annulus.

SINTEF Petroleum Research in Trondheim is conducting a project on hole cleaning performance of oil-based drilling fluids in a flow loop experimental rig with eccentric annulus that closely simulates real well conditions. This presents a great opportunity to conduct a set of experiments on pressure drop in the flow loop and use the experimental data for validation of theoretical predictions. The goal will be to find an approximation that gives good predictions of pressure drop in eccentric annulus.

When calculating the pressure losses it is necessary to provide a mathematical model that correctly describes the rheological behaviour of the fluid in terms of relationship

between shear and stress. The commonly used models are Bingham-Plastic, Power law and Herschel-Bulkley models. These will be tested for fitting with the available oil-based drilling fluids and the best one will be used for further work on pressure drop estimation.

The experiments are planned to be conducted by SINTEF Petroleum Research, among which also pressure drop experimental data are to be measured. In order to be able to conduct these, the rheology of the fluid in the flow loop has to be stable throughout the duration of the project to enable comparison of the experimental results with the rheological data from the fluids used. In order to verify the rheological stability of the fluids in the flow loop, the rheology needs to be measured periodically through the course of the semester to keep track with the changes and to be able to maintain the required viscosity profile.

For the periodic measurements, API recommended practices are to be used for the measuring procedure. These, however, do not specify in detail how the fluid samples should be pre-treated before measurements. The pre-treatment of samples and few other factors that can affect the quality of the measurements will be studied in order to enable correct evaluation of the quality of our results. This will be included in a separate chapter.

2. Fundamental theory

2.1. Basics of rheology

Rheology is the study of the flow and deformation of matter under the effect of an applied force. Rheology is applicable to all materials, from gases to solids. But in practice, as Figure 1 shows it is principally concerned with extending the relatively straightforward disciplines of elasticity and Newtonian fluid mechanics to more complicated and realistic materials, developing fundamental relations between force and deformation.

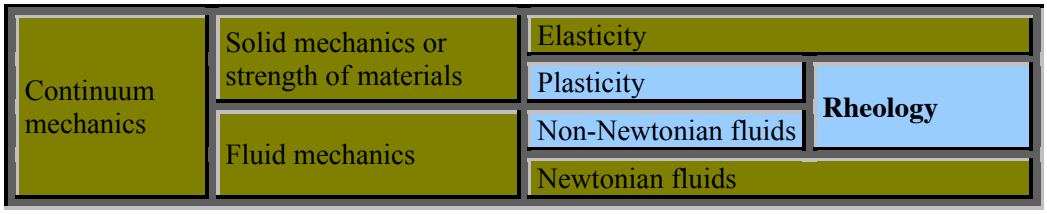

Figure 1: Main focus of rheology

Shear stress

Shear stress τ is defined as force applied to a sample, expressed as force per area:

$$\tau = \frac{F}{A} \, [Pa] \tag{1}$$

Shear rate

Shear is sliding deformation that occurs when there is movement between layers in a sample. Expressed as the amount of movement that occurs in a given sample dimension this becomes dimensionless. Shear rate is then expressed as velocity of a fluid layer relative to another layer divided by the distance between them:

$$\dot{\gamma} = \frac{du}{dy} \, [s^{-1}] \tag{2}$$

Viscosity

Viscosity is the measure of a fluids resistance to deformation under stress and is defined as the ratio of shear stress to shear rate:

$$\mu = \frac{\tau}{\dot{\gamma}} \, [Pas] \tag{3}$$

Viscosity is a property that can be expressed by a coefficient for some fluids (see Newtonian), while for other it is a function of shear rate.

Viscoelasticity

Viscoelasticity is a property of materials that exhibit both viscous (liquid like) and elastic (solid like) characteristics, such as drilling fluids for instance. Storage modulus G' and the loss modulus G'' are two parameters that describe the viscoelastic behavior of a fluid. The storage modulus represents the elastic behavior of the material and is a measure of the deformation energy stored by the material under shear. If this energy is completely stored in the material while it is subject to shear strain, then the material will return to its original structure once the strain is removed. The loss modulus represents the viscous behavior of the material and is a measure of the deformation energy dissipated as heat under shear.

2.2. Potential rheological models

Rheological models describe fluids mathematically by their rheological behaviour (Figure 2). Fluids can be divided into two main groups depending on their response to shearing: Newtonian and non-Newtonian. The first group shows a direct proportionality between shear stress and shear rate, the other does not. Most drilling fluids are non-Newtonian fluids, with viscosity decreasing as shear rate increases.

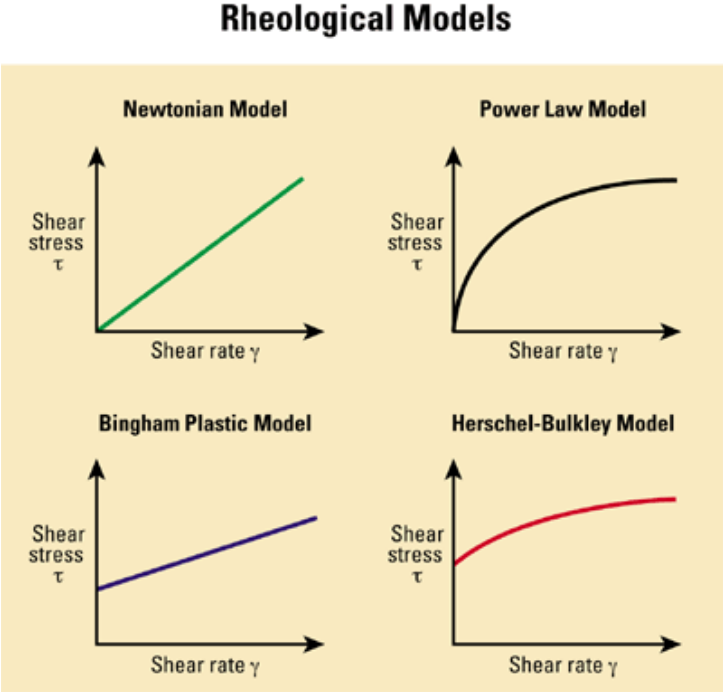

Figure 2: Rheological models (Schlumberger 2015)

Newtonian

The Newtonian model describes fluids with constant viscosity, which is independent of shear rate and the time of shearing, provided that temperature and pressure stay constant. Examples are water and base oil. Newtonian fluids are described by the following relationship:

$$\tau = \mu * \dot{\gamma} \tag{4}$$

The shear stress of a Newtonian fluid is proportional to the shear rate, and viscosity μ represents the constant of proportionality.

Bingham Plastic

Some fluids require a certain minimum stress to initiate flow, given as yield point τ_y in the Bingham Plastic model. After exceeding this yield point, the fluid behaves like a Newtonian fluid for increasing shear rate.

$$\tau = \tau_y + \mu_{pl} * \dot{\gamma} \tag{5}$$

Examples are toothpaste and mayonnaise.

Power Law

Power law fluids are defined by the following equation:

$$\tau = K * \dot{\gamma}^n \tag{6}$$

where K is the consistency index and n is the flow behaviour index. In essence, K is the viscosity (or stress) at a shear rate of 1 s^{-1} and n is a measure of non-Newtonian-ness of a fluid. Depending on the value of n, the model describes three types of fluids:

$n = 1$ Newtonian fluid

$n > 1$ dilatant fluid (shear thickening)

$n < 1$ pseudoplastic fluid (shear thinning)

Herschel-Bulkley

Herschel-Bulkley model is the one that is used most in describing drilling fluids, as it takes into consideration all of the aforementioned parameters:

$$\tau = \tau_y + K * \dot{\gamma}^n \tag{7}$$

The constants K and n are the same as for the Power law model; the yield point is the same as for Bingham model. If τ_y is zero, the Herschel-Bulkley model reduces to the Power law model. When n is one, the model is reduced to the Bingham Plastic model. When designing the viscosity curve of a drilling fluid, it must be taken into consideration that the fluid will experience a broad range of shear rates in different sections of wellbore and different situations (high, low or no circulation). That is the reason of popularity of the Herschel-Bulkley model, which is suited to describe the behaviour of a drilling fluid for any shear-rate.

2.3. Oil-based drilling fluids

Oil-based drilling fluids consist of oil, which is the continuous phase, and water that is the dispersed phase. The system is called an emulsion, which is defined as dispersion (droplets) of one liquid in another immiscible liquid. The amount of water emulsified in the oil can vary between 5-50% for drilling fluids (UiS 2011), but can else range from less than 1% and greater than 80% (Petrowiki 2015). In order to inhibit the different phases from separating from each other by merging and forming

two separated continuous phases, it is important to keep the emulsion stable. The method most often used for the drilling fluids is called “steric stabilization”, by use of an emulsifier, which coats the water droplets and prevents them from aggregating. This will not prevent the phases from gravity separation when left to rest for several days (as was observed on stored fluid samples), but the emulsion stability is not diminished. By shearing the fluid at high shear rate the fluid is brought back to its initial condition.

2.3.1. Rheology of oil-based drilling fluids

Fluids that have a viscosity that is time dependent are called thixotropic or rheopectic. Most drilling fluids are thixotropic fluids, meaning that they behave shear thinning and their viscosity decreases when exposed to shear over time. Rheopectic behavior is related to the shear thickening fluids, meaning that their viscosity increases when exposed to shear over time. This property of drilling fluids is important to take into consideration when working with well stability.

The thixotropic behavior is due to a change in the colloidal structure of the fluid under shear. The change is reversible and the structure starts rebuilding, when the fluid is not exposed to any shear or to shear at much lower rates, as can be seen in Figure 32 with further explanation in Ch. 5.3. This process is called aging.

2.3.2. Application of oil-based drilling fluids

The use of oil-based drilling fluids is restricted in many places, since it is often considered more environmentally harmful compared to water based drilling fluids. Drilling with OBDFs has both advantages and disadvantages. One of the advantages is that the OBDFs suppress the hydration of clay, which can occur when drilling through shale layers. An example of the consequences of this reaction between water and clay particles will be described in Ch. 5.1.

2.4. Flow regimes

Considering flow of drilling fluids three distinct flow regimes can describe their approximate behaviour: Laminar flow, turbulent flow and transitional flow. When calculating on pressure losses in a pipe/annulus it is important to know, which of the three regimes the fluid follows. Depending on the geometry of a wellbore all three

flow regimes can exist in the different parts of the well. The pressure drop is then calculated for each of the geometry sections separately, using different equations.

Laminar flow is characterised by smooth layers of fluid in an ordered motion, moving straight and parallel to the walls.

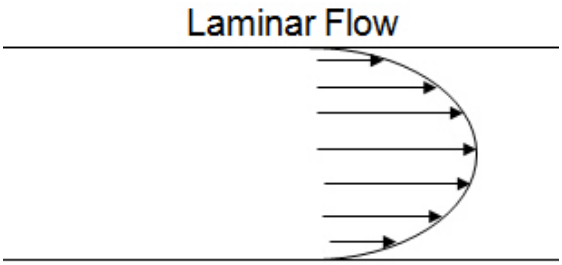

Figure 3: Laminar flow (Drillingformulas 2012)

Turbulent flow is described by a chaotic behaviour that is dominated by random and rapid fluctuations, called eddies.

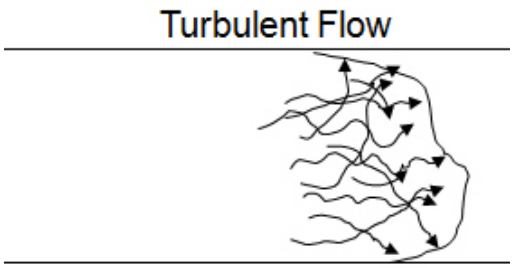

Figure 4: Turbulent flow (Drillingformulas 2012)

Transitional flow describes the transition between laminar and turbulent flow regimes. In the region of transitional flow regime, the flow changes gradually from laminar to turbulent.

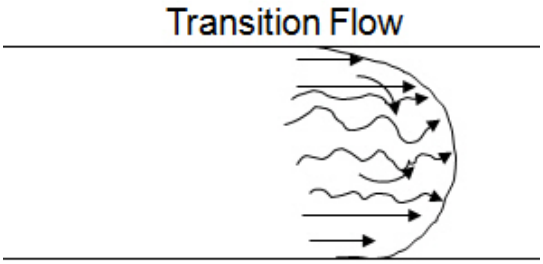

Figure 5: Transition flow (Drillingformulas 2012)

In 1883, when Mr. Osborne Reynolds did the fluid study, he discovered Reynolds number describing flow of water in a circular pipe (Drillingformulas 2012). According to this number it was possible to predict, in which regime the fluid was flowing. For flow in straight circular pipes, the transitional regime was confined to $2300<Re<4000$ (Cengel 2004). Below this region the fluid flow would be laminar; above this region it would be turbulent. For drilling fluids, the definition of these limits is more complex since one has to take into consideration the thixotropic property of the fluids, as will be seen in Ch. 3.2.4.

2.5. Viscosity and elasticity measurements

Rheological measurements are normally performed in kinematic instruments in order to establish the viscosity profile of a fluid and elastic properties, such as gel strength and yield point value.

A viscometric measurement normally consists of a shear rate analysis, also called flow curve test. The flow curve test is a rotational test that covers a range of shear rates that the fluid of interest is expected to be exposed to, usually from 1 to 1200 s^{-1}.

A rheometric measurement normally consists of a strain or a stress analysis at a constant frequency (normally 1 Hz). The Amplitude sweep test (strain sweep test) is an oscillatory test that gives information of the elastic modulus G', the viscous modulus G'' (Figure 6). It is used to determine the linear viscoelastic region (LVER). The Amplitude sweep shows how the applied strain affects the sample: Where the colloidal structure begins to break down and how quickly it breaks down. Before this breakdown the fluid is in the LVER (constant G' and G''), and that is where all other tests are done.

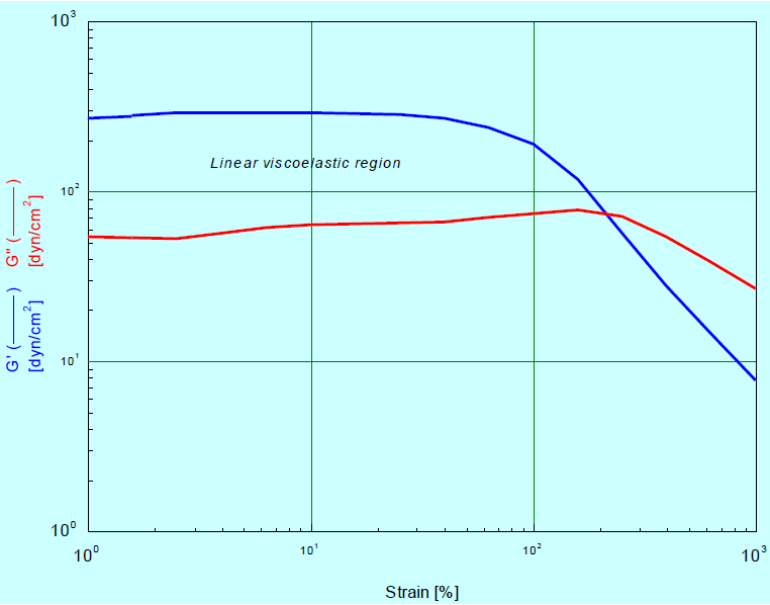

Figure 6: Example of Amplitude sweep test (Clark 2015)

3. Flow loop investigations – Theory and results

3.1. Rheological stability of the fluid in the flow loop

In order to be able to conduct any experiments in the flow loop experimental rig, the rheology of the fluid in the active system had to be measured periodically. The experiments were conducted in the course of the whole semester, among which also pressure drop experimental data were measured. The rheology had to be stable to enable comparison of these experimental results with rheological data on the fluids used. The fluid in the active system was changed several times during the scope of the thesis, but the experiments were conducted while their rheology remained stable. The different drilling fluids have got different names. Both the experimental rig and the tested fluids are described more thoroughly in the following subchapters.

3.1.1. Experimental facilities - The flow loop experimental rig

The basis of all the conducted experiments on different drilling fluids is the flow loop experimental rig (Figure 7). All the fluid samples used in this thesis were collected from this experimental rig.

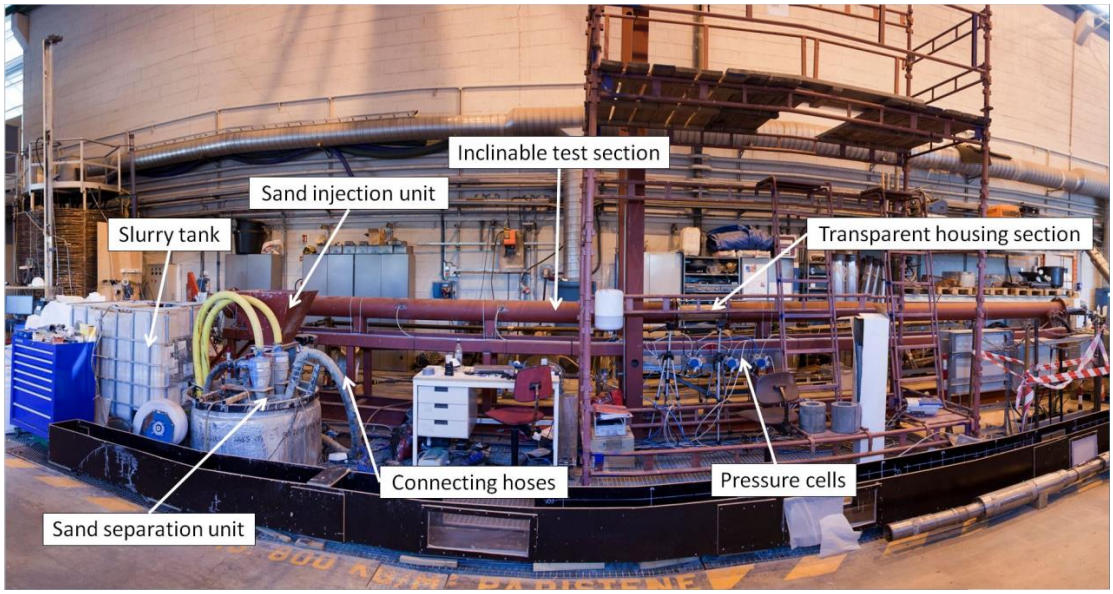

Figure 7: Flow loop experimental rig, courtesy of Werner (2014)

The actual set-up of the flow loop has been modified in the process of the project, but the modifications were not influential for the purpose of this thesis. During the scope of the whole project conducted by SINTEF Petroleum Research, borehole hydraulics,

torque and hole cleaning aspects were investigated (Taghipour 2014). The test setup was realistic in terms of components it consisted of. The experiments were conducted at ambient pressure and temperature, as it was considered sufficient for the purpose of the study. The main controllable parameters were liquid velocity, string rotation and sand injection rate.

The experimental rig consists of the following main components:

- Test section
- Liquid slurry unit
- Sand injection unit
- Sand separation unit
- String rotation motor
- Instrumentation
    - Pressure cells
    - Load cell
    - Flow meter

The test section (Figure 8) is a 10.3 meter long cylindrical housing for the wellbore and the drill string. It is inclinable up to 30° from horizontal position. The inner side consists of 4" ID replaceable hollow wellbore segments made of concrete with circular geometry. Non-circular geometry was as well applied earlier in the project, but not for the experiments of this thesis. A 2" OD steel rod is placed eccentrically inside the test section and used in free whirling mode to imitate a drill string in natural dynamic motion in the borehole. This was achieved by connecting the rod to a 4 kW drive motor with gear box at one end of the test section and using flexible joints to connect the rod to a load cell on the other end. The key parameters of the test section are given in Appendix A.

Figure 8: Test section, 10.3 meters long

The liquid slurry unit consists of a slurry tank and a pump. The slurry tank has a volume of 1 m^3 and is connected to a mixing tank, where the drilling fluid is prepared. The pump, which is driven by an electrical polyphase motor, is connected to the tank and drives the fluid around the flow loop. A flow meter is installed between the test section and the slurry tank in order to be able to measure the fluid velocity.

Sand is used to represent cuttings in the experiments of the project, related to hole cleaning investigation. It is injected through a dry sand injection unit at a controlled rate into the slurry tank, from where the fluid enters the test section. It is separated out when the fluid passes through the sand separation unit, before it enters a collection tank. From there the fluid is recirculated into the test section. The experimental study of the following thesis focuses on the aspects that concern the rheology of the fluids and their rheological behaviour. Hence, all the measurements conducted for this work are done on flow without any sand in the system and with no string rotation. A more detailed description of the sand treating units and the string rotation motor is therefore omitted.

The instrumentation systems consist of several differential pressure (DP) transducers, temperature gauges and an electromagnetic flow meter, connected to a digital logging system. This is operated from a computer with customized logging software. The temperature gauges keep track of the temperature in the active system. The DP cells measure the differential pressure at 1 m, 4.2 m and 10.3 m distances inside the test section, and will be described in more detail in Ch. 3.2.

3.1.2. Test fluids

The fluid systems that were used for the project were delivered by M-I SWACO. These were oil-based drilling fluids (OBDF) that had been used during real drilling operations, with densities of 1.28 and 1.5 g/ml, and the corresponding base oil. Prior to use in the experimental rig, the fluids were cleaned, reconditioned and characterized by their density, oil-water-ratio (OWR) and viscosity profiles.

- Versatec 1.28 sg
- Versatec 1.50 sg
- EDC 95/11 (base oil)

The fluids were further adjusted (as shown below) to provide test fluids with the following specifications:

- OBM A = Versatec 1.28 sg diluted with EDC 95/11 to sg 1.11
- OBM B = OBM A mixed with Versatec 1.50 sg to 1.26 sg
- OBM C = OBM B + Bentone 128 (viscosifier)

OBM A, OBM B and OBM C drilling fluids were used for the experiments in this thesis. The exact compositions are not specified due to commercial restrictions. The only available information is the OWR value and the general compositional background of the basis fluid, Versatec:

- Oil-water ratio: 80/20
- Weight material (barite)
- Salts ($CaCl_2$)
- Organophilic clay (bentonite)
- Lime ($Ca(OH)_2$)
- Emulsifier (ethanol compound)
- Fluid loss agent (Versatrol)

These test fluids had specific viscosity profiles that made it possible to compare the results achieved in the following campaign with the results made in earlier campaigns. As the names suggest, all of the mentioned fluids are oil-based. Earlier campaigns of the project had the same experiments with identical procedures, but on water-based drilling fluids. The identical conditions and viscosity profiles were chosen to make it

possible to draw good conclusions from a comparative study of oil-based and water-based drilling fluids.

3.1.3. Test matrix - Periodic measurements of the active fluid rheology

The viscosity profile and gel strength of the fluid, collected from the main tank of the flow loop, were measured periodically by the Model 35 Fann viscometer (Figure 16), which is a de facto standard method for rheology characterization in the oil industry. Electrical stability (ES) was measured by OFITE Emulsion Stability Tester (Figure 9). At times of intensive experimentation or modifications to the fluid system in the flow loop measurements were taken almost every day, with exception of weekends. Less frequently, when no experiments were conducted or some problems occurred in the test set-up, as for instance in February, when the flow loop experienced some technical problems with the mesh in the sand filtration unit.

Figure 9: OFITE Emulsion Stability Tester (Ofi Testing Equipment 2014)

The measurements in the test matrix (Table 1) were done for all fluid systems, initially at 28ºC and later at 50ºC as well (for OBM B and OBM C). The viscosity profile and gel strength of the fluid provided information about rheological stability of the fluid in the flow loop. The ES value, a property of oil-based drilling fluids related to its emulsion stability and oil wetting ability, provided information related to the value of the actual oil-water ratio of the fluid.

Temperature [ºC]	**Fann 35 viscometer, RPM**						**Gel strength**		**ES**
	3	6	100	200	300	600	10 sec	10 min	**[V]**
Fluid name									

Table 1: Test matrix for the rheology measurements.

3.1.4. Test results – Verification of rheological stability of the active fluid

The periodic measurements of the fluid rheology showed that the viscosity profiles remained stable and allowed running of experiments for OBM A and OBM B. OBM C experienced some problems with decreasing viscosity profile. Therefore, the values in the Tables 2-3 show some fluctuations. The problem was found and dealt with, and is described in detail in Ch.5.1.

28°C	Fann viscometer, RPM						Gel strength		ES
	3	6	100	200	300	600	10 sec	10 min	[V]
OBM A	3	3.5-4.0	11	17	22.5	39.5	x	x	784
OBM B	4	4.5	15	24	33	58	x	x	870
OBM C	5.5-7.0	6.0-8.0	25-28	34-37	55-59	94-100	10-11	21-22	1402-1999

Table 2: Measurements for verification of rheological stability of the test fluids at 28 °C.

50°C	Fann viscometer, RPM						Gel strength		ES
	3	6	100	200	300	600	10 sec	10 min	[V]
OBM A	x	x	x	x	x	x	x	x	784
OBM B	4	5	12	17.5	22	35	x	x	870
OBM C	6.0-7.0	6.5-8.0	18-20	27-29	37-39	61-64	8.0-9.0	18-20	1402-1999

Table 3: Measurements for verification of rheological stability of the test fluids at 50 °C.

The complete overview of these measurements can be found in Appendix B. These include measurements mainly from the main tank of the flow loop, but also some measurements for fluids from storage tanks. The latter are the values that do not appear chronologically in the table.

3.2. Pressure drop in the annulus and its theoretical estimation

Before any experiments can be started and the pressure drop measurements can be taken, steady state conditions had to be achieved in the flow loop. A constant flow rate was reached after choosing one of the velocity settings. The logging system kept track of the different parameters. The flow was circulated until steady state (stable pressure gradient) in the flow system is achieved. Then the experiments were conducted.

Pressure drop in the flow loop was measured by differential pressure cells that are connected via hoses to the test section and are filled with water in order to transmit the pressure. These measure the differential pressures at distances of 1 m, 4.2 m and 10.3 m inside the test section, as depicted in Figure 10 and described in Table 4.

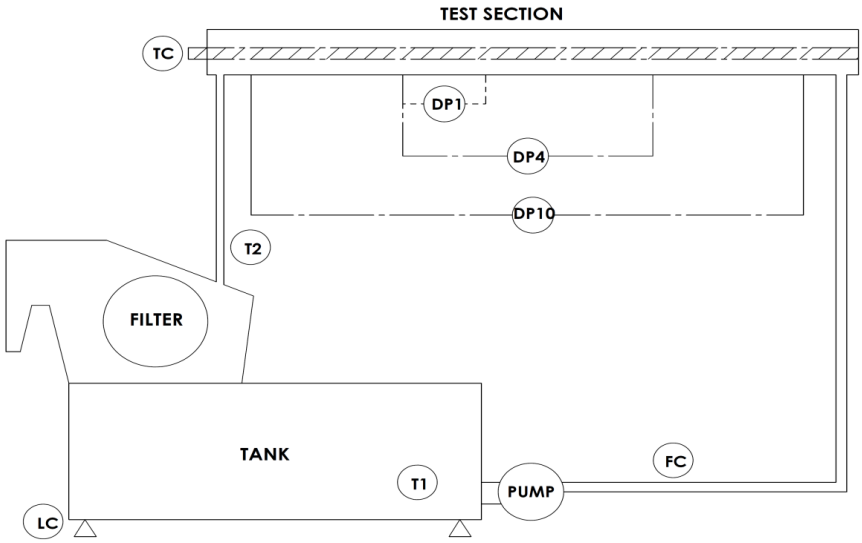

Figure 10: Flow diagram of the instrumentation on the flow loop experimental rig (Lund et al. 2015)

Sensor	Measuring parameter	Dimension
DP1	Differential Pressure in 1 meter	mbar
DP4	Differential Pressure in 4.2 meters	mbar
DP10	Differential Pressure in 10.3 meters	mbar
TC	Torque cell inner rod	Nm
T1	Temperature inside the main tank	ºC
T2	Temperature at test section outlet	ºC
LC	Load cell (Tank weight)	Kg
FC	Flow meter	m/s

Table 4: The different components of the instrumentation in Figure 10.

The pressure drop data used in this work were taken from the DP4-cell, which measures the differential pressure over a distance of 4.2 meters, starting approximately at 3 meters from the entrance of the test section. In this way we are eliminating the potential entrance and exit effects on the pressure data that are present in the DP10-cell and reducing the chance of potential measurement noises in DP1-cell, which is expected to be affected by these more than the DP4-cell. Another reason for using the DP4-cell is the least value of the measured pressure offset, when compared to the DP10-cell (Figure 11). Offset is a measure of disturbance in pressure data that needs to be compensated when calculating pressure drop. It is measured at very slow axial velocities. Figure 11 shows offset for a range of velocities, and it is constant because velocity gradient is very small. A zero-velocity offset (pressure drop) is estimated for the relevant pressure cells. More on the evaluation of the pressure offset effect in Ch. 5.2.

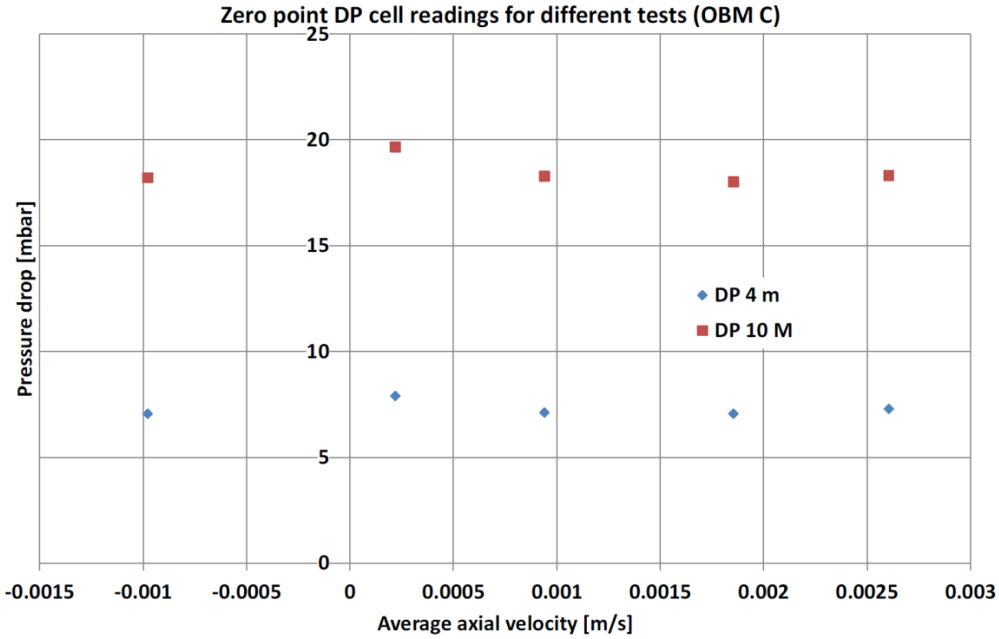

Figure 11: Pressure offset in flow loop measurements, DP4-cell and DP10-cell (Lund et al., 2015)

3.2.1. The approach

One of the goals of this thesis was to find a theoretical method to predict the pressure losses in the annulus of the available flow loop experimental rig, where the differential pressure data were measured and could be used for comparison purposes.

The reviewed literatures provided different solutions and approximations, so it was necessary first to find out what we dealt with. The focus was laid on the fluids tested and the conditions they were exploited under.

The laboratory at the "Department of petroleum engineering and applied geophysics" provided different testing equipment, among which Anton Paar rheometer (Figure 17) was found to be ideal for the purpose of characterization of the fluids. The rheometer provided oscillatory and rotational tests with very high precision.

Two fluid systems were tested in the Anton Paar rheometer, OBM B and OBM C. First, several samples of each of the fluids were used for determination of flow curves (see Ch. 4). Later, these flow curves were analysed by Rheoplus, the software of the rheometer. The analysis method used is called Auto-Regression, which can be used to try out a number of models on the measurement results. The control panel is shown in Figure 12. The software checks the fitting of the selected models and chooses the one with the best correlation. As a result the name and equation of the best-fitting model are shown with the calculated regression parameters. The two models that were relevant for the oil-based drilling fluids are Bingham plastic model and Herschel-Bulkley model.

The Bingham plastic model describes the flow curve of a material with a yield stress and a constant viscosity (Newtonian behaviour) at stresses above the yield stress. The Herschel-Bulkley model describes the flow curve of a material with a yield stress and a shear thinning or shear thickening behaviour at stresses above the yield stress. The Power-law model, frequently used in the industry, is covered by the Herschel-Bulkley equation. This was obtained by setting the yield stress value to zero, and is therefore omitted in the list of the available models.

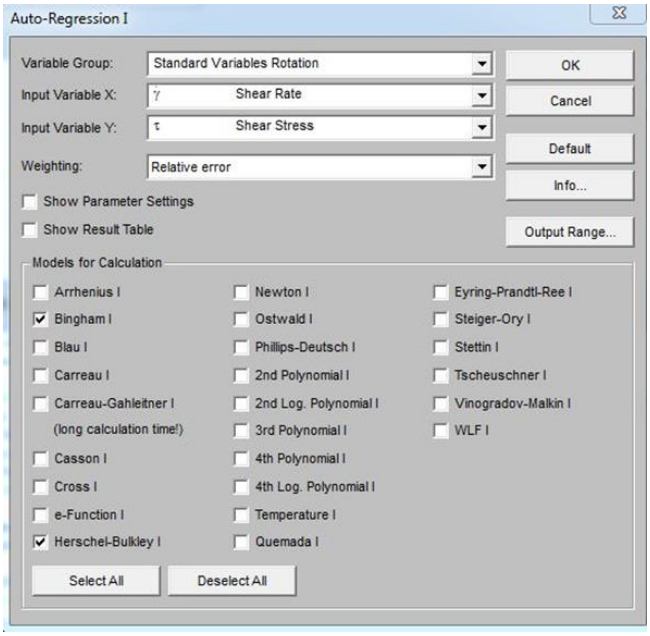

Figure 12: Auto-Regression - parameter settings (Rheoplus software 2015)

The analysis tool provided Herschel-Bulkley model as the one that fitted best to the measurement data for all the cases of different samples of OBM B and OBM C fluid systems. Some of the measurement results from Fann 35 viscometer are given in Figure 13 together with the chosen rheological model and corresponding equation parameters to illustrate the suitability.

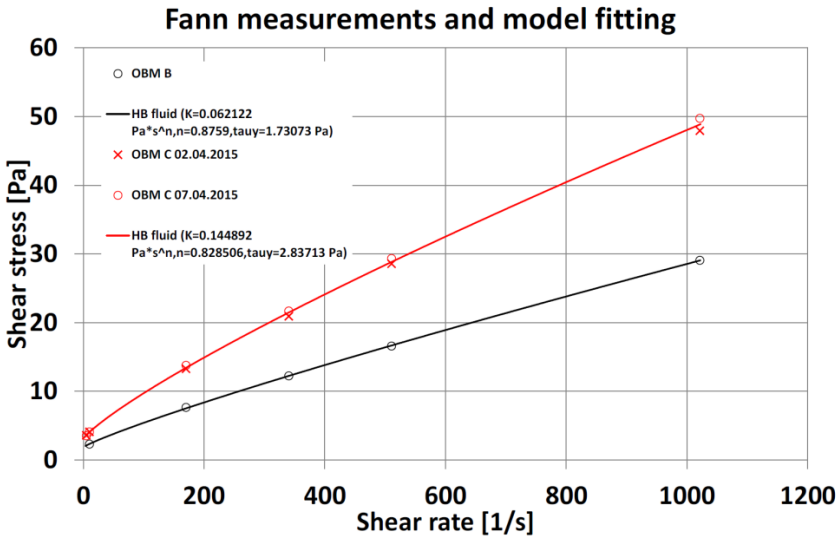

Figure 13: Herschel-Bulkley model fitting for Fann 35 measurements (Lund et al. 2015)

With this, it was concluded that OBM B and OBM C are Herschel-Bulkley fluids.

The next step was to define the flow regimes that were created in the flow loop in the conditions that the test fluids were subjected to. This was essential for defining the method of estimating the pressure drop in the annulus. The reviewed literature differentiated between analytical, semi-analytical and numerical methods, depending on the flow regime. Reynolds number (Re) was calculated for each case of the relevant experiments and it was shown that Re was lower than the lower limit of transitional flow regime (Eq. 24) for each case. This finding defined the focus of the literature review on solutions for the laminar flow regime, presented in the following subchapter.

3.2.2. Existing theoretical methods

The focus of the literature review was theoretical methods that regard Herschel-Bulkley drilling fluids in laminar flow conditions through eccentric annuli. Most of the reviewed literature combined different solutions published earlier with own theoretical and numerical analysis and experimental measurements into one consistent method of calculating pressure drop over the entire range of flow regimes. Examples of such works are of Founargiotakis et al. (2008), Pilehvari and Serth (2009) and Reed and Pilehvari (1993).

Founargiotakis et al. (2008) developed an integrated approach for prediction of pressure drop for laminar, transition and turbulent flow in concentric annuli. For the laminar region of flow prior analytical solutions were used. The approach was tested on experimental data from other previous works showing good match. The same experimental data from Okafor and Evers (1992), Langlinais et al. (1983) and Fordham et al. (1991) have been used to verify the Narrow slot approximation method derived in the next subchapter for regions of laminar flow in the process of the derivation. The predicted pressure drop values showed good agreement for the laminar flow region. The verification data and results are not included in this work. These were used only for validation purposes of the equations derived.

Laminar flow of Herschel-Bulkley fluids in concentric annulus has been investigated by Hanks (1979), who provided a non-analytical solution, although with some errors pointed by Buchtelova (1988). Hansen et al. (1999) presented a model for laminar

flow in annuli, constructed by theoretical and numerical analysis and experimental measurements. Fordham et al. (1991) provided a method with numerical solution and some experimental laminar flow data for Herschel-Bulkley fluids. Kelessidis et al. (2006) provided a comprehensive solution for Herschel-Bulkley fluid flows in concentric annuli covering laminar flow.

Of all these works, the slot model approach used for approximation of flows in concentric annuli by Kelessidis et al. (2006) will be used in the present approach.

3.2.4. Narrow slot approximation method for pressure drop estimation in eccentric annulus

The aim of this part of the thesis was to find a theoretical method that predicted the pressure losses in an eccentric annulus.

The solution that will be derived follows the procedure of Kelessidis et al. (2006), which provides a relationship between flow rate and pressure drop for Herschel-Bulkley drilling fluids flowing in laminar flow in concentric annuli, modelled as a slot. The work provided a solution, where the flow rate can be directly determined given the pressure drop. But trial-and-error solution is required if the pressure drop is to be determined for a given flow rate. The expressions were derived further by Lund (2014) to present the pressure drop as a function of the average wall shear stress. The implicit equation for the wall shear stress was solved numerically by a designed MATLAB program (Appendix C).

The relationship between the average fluid velocity U and the average wall shear stress $\overline{\tau}_w$ can in the narrow-slot approximation for Herschel-Bulkley fluids be expressed as (after Aadnoy et al. 2009):

$$\frac{12U}{D_o - D_i} = \frac{(\overline{\tau}_w - \tau_y)^{\frac{n+1}{n}}}{K^{\frac{1}{n}}\overline{\tau}_w{}^2}\left(\frac{3n}{1+2n}\right)\left(\overline{\tau}_w + \frac{n}{1+n}\tau_y\right) \tag{8}$$

where τ_y is the yield stress, K is the consistency index and n is the flow index.

The average wall shear stress is related to the pressure gradient by:

$$\frac{dp}{dx}A = \overline{\tau}_w P \tag{9}$$

where A is the cross sectional flow area and P is the wetted perimeter

$$\begin{aligned} A &= \frac{\pi}{4}({D_o}^2 - {D_i}^2) \\ P &= \pi(D_o + D_i) \end{aligned} \tag{10}$$

Thus

$$\frac{dp}{dx} = \frac{2\overline{\tau}_w}{\delta} \tag{11}$$

where δ is the annular gap for a concentric annulus

$$\delta = \frac{1}{2}(D_o - D_i) \tag{12}$$

The above formula can be rewritten, using the definition

$$\xi = \frac{\tau_y}{\tau_w} \tag{13}$$

Then

$$\frac{6U}{\delta} = \frac{\left(\overline{\tau}_w - \tau_y\right)^{\frac{n+1}{n}}}{K^{\frac{1}{n}}\overline{\tau}_w}\left(\frac{3n}{1+2n}\right)\left(1 + \frac{n}{1+n}\xi\right) \tag{14}$$

Rearranging, we obtain

$$\overline{\tau}_w = \left(\frac{2U}{\delta}\right)^n (1-\xi)^{-(n+1)}\left(\frac{1+2n}{n}\right)^n \left(1 + \frac{n}{1+n}\xi\right)^{-n} \tag{15}$$

With some further rearrangements this becomes

$$\tau_w = f * \frac{1}{2}\rho U^2 = \left\{\frac{2K^{\frac{1}{n}}(n+1)U}{\delta n(1-\xi)^{1+1/n}\left[(1-\xi)\frac{n+1}{2n+1} + \xi\right]}\right\}^n \tag{16}$$

This implicit equation (16) is programmed and solved in MATLAB.

Further, the effective viscosity μ_{eff} defined as the viscosity that gives the same pressure gradient as a Newtonian fluid at the same flow rate (average velocity, U). In the narrow slot approximation:

$$\frac{dp}{dx} = \frac{12\mu U}{\delta^2} \tag{17}$$

The pressure gradient for a Herschel-Bulkley fluid is, in the narrow slot approximation

$$\frac{dp}{dx} = \frac{2\tau_w}{\delta} = \frac{2K}{\delta}\left\{\frac{2(n+1)U}{\delta n(1-\xi)^{1+1/n}\left[(1-\xi)\frac{n+1}{2n+1}+\xi\right]}\right\}^n \tag{18}$$

Thus

$$\mu_{\text{eff}} = \frac{\delta K}{6V}\left\{\frac{2(n+1)U}{\delta n(1-\xi)^{1+1/n}\left[(1-\xi)\frac{n+1}{2n+1}+\xi\right]}\right\}^n \tag{19}$$

Defining the corresponding effective Reynolds number

$$Re_{\text{HBeff}} = \frac{\rho U D_h}{\mu_{eff}} \tag{20}$$

where D_h is the hydraulic diameter

$$D_h = \frac{4A}{P} \tag{21}$$

In the narrow slot approximation

$$D_h = 2\delta \tag{22}$$

$$Re_{HBeff} = \frac{12\rho U^2}{K\left\{\frac{2(n+1)U}{\delta n(1-\xi)^{1+1/n}\left[(1-\xi)\frac{n+1}{2n+1}+\xi\right]}\right\}^n} \tag{23}$$

Guillot (1990) has suggested to use the limits of transitional region of the flow from (Dodge and Metzner 1959) that give the lower limit of Re, at which transition occurs as:

$$Re_{lower} = 3250 - 1150n' \tag{24}$$

where n' is the local power law value of n.

Analytical solutions for the flow of non-Newtonian fluids and particularly for Herschel-Bulkley fluids in eccentric annuli for laminar flow do not exist (Kelessidis et al. 2011). Hence, resort should be made to correlations. The correlations that most of the bibliography on the topic refers to were proposed by (Haciislamoglu et al. 1990; 1994). The authors solved numerically the equations of motion for axial laminar flow of power-law fluids. The results were presented in the form of a regression equation for the ratio, R, of pressure gradient in an eccentric annulus to that in a concentric annulus:

$$(\frac{dP}{dl})_{eccentric} = R * (\frac{dP}{dl})_{concentric} \tag{25}$$

It was shown that R in a uniformly eccentric annulus in laminar flow is a function of eccentricity, e, flow behaviour index, n and pipe diameter ratio, $\frac{D_i}{D_o}$, and can be calculated with the correlation below:

$$R_{lam} = 1 - 0.072\frac{e}{n}\left(\frac{D_i}{D_o}\right)^{0.8454} - 1.5e^2\sqrt{n}\left(\frac{D_i}{D_o}\right)^{0.1852} + 0.96e^3\sqrt{n}(\frac{D_i}{D_o})^{0.2527} \tag{26}$$

The eccentricity is defined as the distance between two pipe centres divided by the gap. In the experiments of this thesis the eccentricity was 1, i.e. with the inner and outer pipes touching each other.

Eq. (26) is valid for the following parameter ranges: $0.3 \leq \frac{D_i}{D_o} \leq 0.9$, $0 \leq e \leq 0.95$ and $0.4 \leq n \leq 1.0$ within the accuracy (5%) of the correlation (Pilehvari and Serth 2009).

The range for $\frac{D_i}{D_o}$ covers most practical applications, and the correlation can be extrapolated to include the fully eccentric annulus (e = 1.0) with little error.

3.2.5. Test matrix - Pressure drop in eccentric annulus

In order to check how well theoretical estimation values match the experimental pressure drop data the simplest form of the experiments was sufficient. This is represented by experiments without any string rotation or sand in the flow loop. As reported by (Ytrehus et al. 2014), for the eccentric case the string rotation causes inertial effects, which tend to increase the pressure gradient. For a fully eccentric case this may dominate the shear thinning effects, which reduces the pressure gradient. In the absence of particles and any external forces the hydraulic behaviour of the fluids is represented more accurately. In addition, the geometry of the test section is horizontal. In this way the hydrostatic pressure does not need to be taken into account in the calculations.

The experiments were conducted by measuring pressure drop values for different flow velocities.

3.2.6. Test results – Estimation of pressure drop in eccentric annulus

In this section experimental data for pressure drop in the eccentric annulus were retrieved from the flow loop, Tables 5-6. These were compared to the theoretical estimations (Appendix D) derived in Ch. 3.2.4. As Figure 14 and Figure 15 show, the estimation gives a good match with the experimental data. The set of flow velocities, at which the pressure data were measured, for OBM B and OBM C, were changed in the process of the project due to modifications to the set-up. This had no impact on the results presented here. Each test was done twice in order to verify reproducibility. After confirming the reproducibility of the results, only one set of the test data was used in the calculations of this work.

The measured pressure drop values for OBM B and OBM C:

Flow velocity	Sand Rate	RPM	DP4m	Inlet T	Outlet T	Density	Pressure gradient
[m/s]	[g/s]	[1/min]	[mbar]	[°C]	[°C]	[g/L]	[Pa/m]
0.55	0	0	14.55	28.47	28.35	1258.05	338.4
0.75	0	0	18.96	28.48	28.39		441.0
1.00	0	0	25.12	28.47	28.46		584.1
1.20	0	0	30.04	28.45	28.56		698.5

Table 5: Experimental pressure data for OBM B, horizontal section, eccentric annulus.

Flow velocity	Sand Rate	RPM	DP4m	Inlet T	Outlet T	Density	Pressure gradient
[m/s]	[g/s]	[1/min]	[mbar]	[°C]	[°C]	[g/L]	[Pa/m]
0.30	0	0	17.28	31.05	30.94	1267,10	411.4
0.50	0	0	21.95	31.07	31.02		522.6
0.70	0	0	26.73	31.08	31.15		636.5
0.90	0	0	32.58	31.05	31.23		775.8
1.10	0	0	38.16	30.97	31.25		908.6

Table 6: Experimental pressure data for OBM C, horizontal section, eccentric annulus.

The estimated pressure drop values for OBM B and OBM C compared to experimental data:

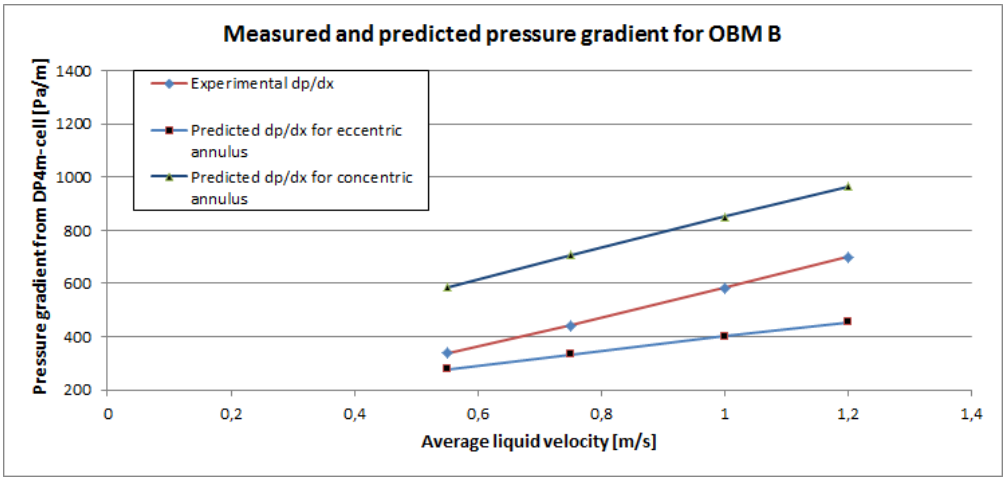

Figure 14: Pressure gradient for OBM B, measured vs predicted (Appendix D) by narrow slot approximation for HB model fluids

The critical Reynolds number, at which transitional flow starts occurring for OBM B was calculated to be 2270. The highest value of Reynolds number for OBM B was calculated to be 1831, at the velocity rate of 1.2 m/s. This proves the validity of the estimation method, which was derived for the laminar flow.

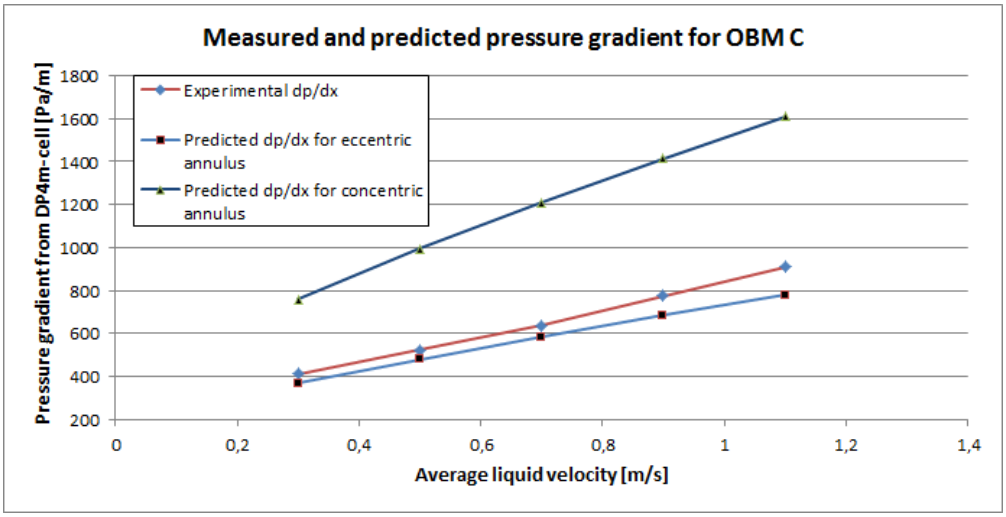

Figure 15: Pressure gradient for OBM C, measured vs predicted (Appendix D) by narrow slot approximation for HB model fluids

The critical Reynolds number, at which transitional flow starts occurring for OBM C was calculated to be 2335. The highest value of Reynolds number for OBM B was calculated to be 923, at the velocity rate of 1.1 m/s. Also in this case the flow was within the boundaries of laminar flow regime.

Evaluation of the predicted pressure drop values:

The narrow slot approximation for HB fluids with correction for eccentricity matches well with the experimental pressure gradients in Figures 14-15. But the slope is different. One of the possible explanations to this is that the equations in the narrow slot model are valid for concentric annuli. This is accounted for by the Haciislamoglu correction factor in the eccentric annulus case. However, the Reynolds number is also calculated for the concentric case and can in reality have higher values. This and other sources of error are further described in Ch. 5.2.

It can be observed that the pressure drop for OBM C is higher than for OBM B. This was expected, due to the higher viscosity of OBM C.

4. Evaluation of the quality and methodology of rheological measurements – Theory and results

Several issues were raised towards the quality of the measurements conducted both with Fann 35 viscometer and Anton Paar Physica rheometer, for the calculations in the last chapter. The ISO 10416/ISO 10414-2 standards, commonly used in the oil industry for determination of rheological properties of oil-based drilling fluids (Fann viscometer), were used for guidance in the execution of some of the tests. These do not in detail specify how the fluids should be pre-treated before measurements. Often, the pre-treatment only consists of simply shearing the fluid sample for a specific amount of time at 1022 s^{-1}, as for example performed by Maxey et al. (2008), who sheared the sample for 2 minutes at their measurement temperature.

In this chapter, a systematic approach is used to quantify the influence of resting time and pre-shearing on measurements of viscosity and other rheological properties of an oil-based drilling fluid (OBDF). OBDFs are thixotropic fluids, meaning that their properties may change with time. As well, OBDFs are highly dependent on shear history. As a result of this, it is important to have a consistent procedure for how to treat the fluids prior to measurements. This is vital for being able to compare experimentally determined flow properties, not only in this study but also to enable comparison of results between labs.

Additionally, an experiment was conducted to try to detect the effect of evaporation at high temperature measurements in Anton Paar Physica rheometer. Further, an experiment was conducted to detect whether a deviation in fluid sample surface level in the measuring cup had any influence on the measurements in the rheometer.

4.1. Experimental background

4.1.1. API recommendations/ISO standards

The standards that are relevant for the experiments of this study are:

1) ISO 10414-2 (API 13B-2)
2) ISO 10416 (API 13I)

Below, relevant extracts from the two standards:

1) API Recommended Practice 13B-2: "Recommended Practice for Field Testing of Oil-Based Drilling Fluids" (API RP 13B-2, 2008)

This standard recommends conducting viscosity and gel strength measurements using a direct-reading viscometer:

- with minimum delay from the time of drilling fluid sampling.
- at either 50 ºC ±1 ºC or 65 ºC ±1 ºC for reference comparisons to historical data

Applying the following procedure:

- Heat the sample to the selected temperature. Use constant shear at 600 rpm to stir the sample while heating to obtain a uniform sample temperature. After the cup reaches the selected temperature, immerse the thermometer into the sample and continue stirring until the sample reaches the selected temperature. Record the temperature of the sample.
- With the sleeve rotating at 600 rpm, wait for the viscometer dial reading to reach a steady value (the time required is dependent on the drilling fluid characteristics). Record the dial reading R_{600}. Follow the same procedure for 300-200-100-6-3 rpm.
- Stir the drilling fluid sample for 10 s at 600 rpm. Stop the rotor and allow the drilling fluid sample to stand undisturbed for 10 s. Record the maximum reading attained after starting rotation at 3 rpm, β_{10s}.
- Restir the drilling fluid sample at 600 rpm for 10 s, stop the motor and allow the drilling fluid sample to stand undisturbed for 10 min. Record the maximum reading attained after starting rotation at 3 rpm, β_{10m}.

2) API Recommended practice 13I: "Recommended Practice for Laboratory Testing of Drilling Fluids" (API RP 13I, 2009)

This standard recommends that the fluid shall be tested after mixing using the techniques in accordance with ISO 10414-2/API Recommended Practice 13B-2.

- Additional measurements: Electrical stability at 50 ºC.

4.1.2. Fann 35 viscometer and general experimental procedure

Fann 35 viscometer (Figure 16) is a direct-indicating viscometer, an instrument used to measure viscosity and gel strength of drilling fluids. There are 6 speeds of rotation, at which viscosity can be measured. These 6 readings define the viscosity profile for the fluid.

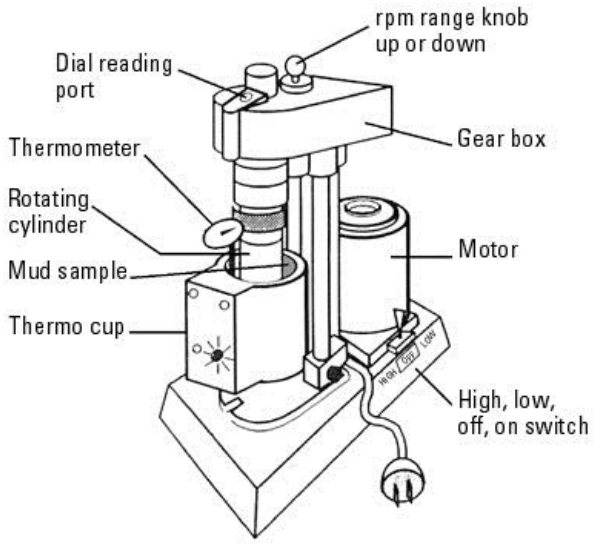

Figure 16: Fann 35 viscometer and Thermocup (Schlumberger, 2015)

An OFITE Thermocup 130-38-25 was used to heat up the fluid samples to the required temperatures. The temperature was at all times observed by use of Eurotherm 2408i Indicator unit, with precision down to 0.01 ºC.

Viscosity and gel strength were measured according to the ISO 10414-2/API Recommended practice 13B-2 (600-300-200-100-6-3 rpm, 10 sec and 10 min gel).

4.1.3. Anton Paar Physica MCR302 rheometer and general experimental procedure

Anton Paar Physica MCR302 rheometer (Figure 17) is a device, which provides oscillatory and rotational tests with high precision. It is equipped with an electrically heated temperature chamber with precision down to 0.01 ºC.

Figure 17: Anton Paar Physica MCR302 rheometer (Anton-Paar 2015)

Figure 18: Hamilton Beach mixer (Etcy, 2015)

Concentric cylinder configuration (Figure 19) was chosen to avoid potential effect of evaporation at 50 ºC.

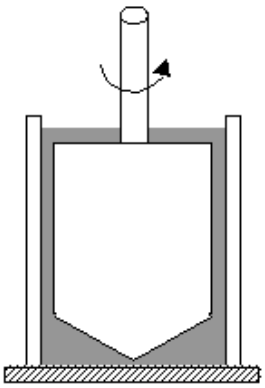

Figure 19: Concentric cylinder configuration (CC27 model)

Experiments that consisted of several measurement sequences (different tests) on the same fluid batch and lasted for several days required a certain preconditioning procedure in order to be able to compare the measurement results from different days. For this purpose, the tested fluid was sheared for 10 minutes at the lowest speed of 13000 rpm on a single spindle Hamilton Beach Commercial 936 mixer (Figure 18) every morning, before a new measurement sequence was started on the Anton Paar MCR Rheometer.

From previous experience (Sandvold 2012), the temperature was expected to increase due to mixing with high rotational speed for a duration of 10 minutes. The temperature in the sample was measured right after mixing (below 30 °C) and did not exceed the maximum recommended temperature for oil based drilling fluids (65 °C) (API RP 13I, Ch.26.3.4).

4.2. Test matrix

All of the following experiments were performed on OBM C drilling fluid.
For a more detailed description of the experiment, see Appendix E.

4.2.1. Experimental study on the effect of resting time and pre-shearing on rheology

The effects of resting time and pre-shearing on measurements were studied using the test matrix in Table 7. For each time interval, measurements were first performed on the rested sample and immediately after repeated on a new rested sample with preceding 10 min with pre-shearing. The measurements were conducted using both Fann 35 viscometer and Anton Paar Physica rheometer at both 28 ºC and 50 ºC.

	Time [hr]	0	1	2	4	6	8	24
Fann 35 viscometer	Resting							
	Resting + 10 min pre-shear							
Anton Paar Physica rheometer	Resting							
	Resting + 10 min pre-shear							

Table 7: Test matrix for Fann 35 viscometer and Anton Paar Physica rheometer.

Fann 35 viscometer measurements

For the Fann 35 viscometer, measurements were started immediately after sampling from the active flow loop ("0 hr"). First, viscosity and gel strength measurements were performed on a sample that was not pre-sheared. Immediately after, the same measurements were performed on a new sample that was pre-sheared for 10 minutes at 600 rpm (equivalent to 1022 s^{-1}). This procedure was repeated for each time interval in Table 7.

Anton Paar Physica MCR302 rheometer measurements

Two sets of experiments were performed with Anton Paar rheometer for each slot in the test matrix, flow curve (rotational test) and amplitude sweep (oscillatory test). Flow curve test (controlled shear rate) measures shear stress values for a given domain of shear rate. As depicted in Figures 26-27, the shear rate values in our tests ranged from 1 to 1200 s^{-1}. An amplitude sweep (Figures 28-31) with a selected range of deformation values and a constant frequency is a test, which is used to find the linear viscoelastic region of the fluid, described in Ch. 2.5. Our tests were performed with a constant frequency of 10 s^{-1} and with increasing strain from 0.001 to 100 %. Both flow curve test and amplitude sweep test were repeated with a 10 min pre-shear at 1000 s^{-1}. Before each test, temperature was set with an accuracy of 0.01 ºC.

4.2.2. Experimental study on the effect of evaporation in Anton Paar rheometer

Performing some of the measurements at 50 ºC, it was brought up several times into discussion during SINTEF meetings, whether there was evaporation and how much it affected the measurement results. The effect of evaporation on measurements was studied by conducting a rotational test with a constant shear rate of 100 s^{-1} for a duration of 1 hour in Anton Paar rheometer. In order to diminish the shear thinning effect of constant shear rate the sample was initially pre-sheared for 10 minutes at 1000 s^{-1}. The test was first done at 50 ºC and was later repeated for 10 ºC. For reasoning, see Ch. 5.3.

4.2.3. Experimental study on the effect of different fluid surface levels in the measuring cup in Anton Paar rheometer

The effect of different fluid surface levels in the measuring cup of Anton Paar rheometer was studied because the measuring cup only holds 17.5 ml of sample. Concerns were raised whether small deviations in the fluid surface level had any impact on the measurements, due to the small total volume of sample. The experiment was conducted by performing a flow curve test with shear rates from 0 to 1200 s^{-1}. First, a test was performed with a sample filled 5-6 mm below normal measuring level (Figure 20). Then, a pipette was used to fill the cup with additional 5-6 mm till the normal line (Figure 21), and the test was performed again.

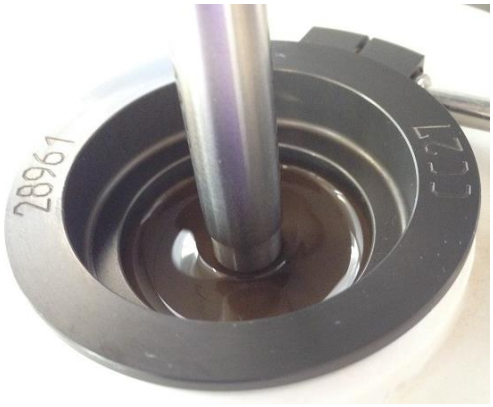

Figure 20: Filled to 5-6 mm below normal line

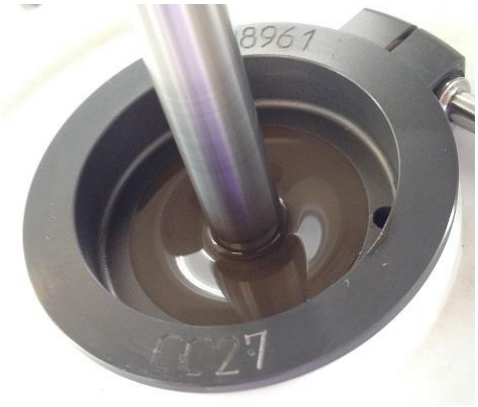

Figure 21: Filled to normal line

4.3. Test results

4.3.1. The effect of resting time and pre-shearing on rheology

Fann 35 viscometer measurements at 28 ºC:

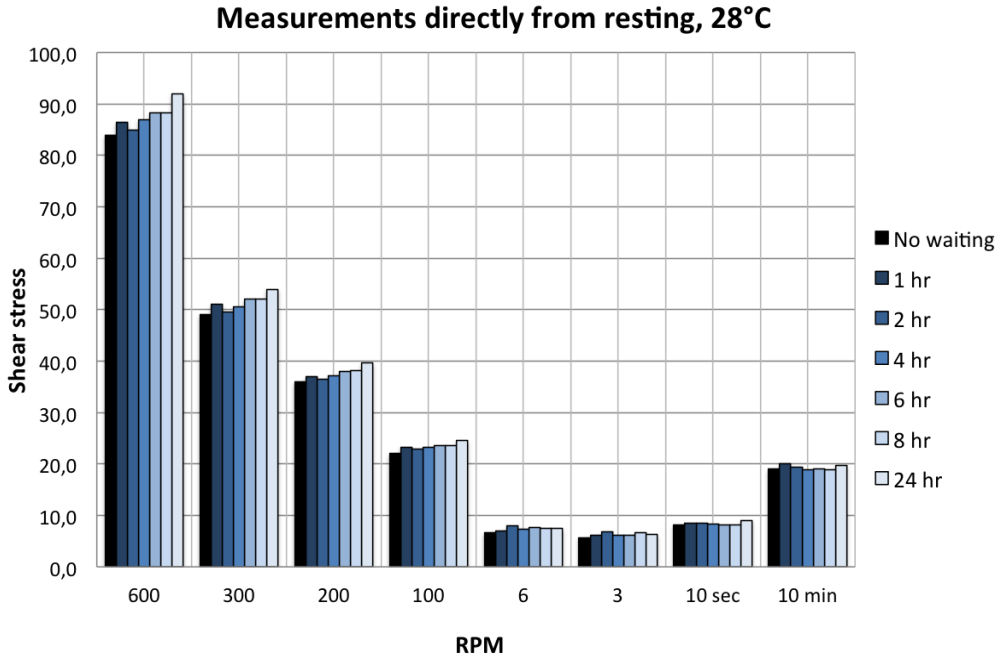

Figure 22: Fann 35 measurements on rested samples at 28 ºC

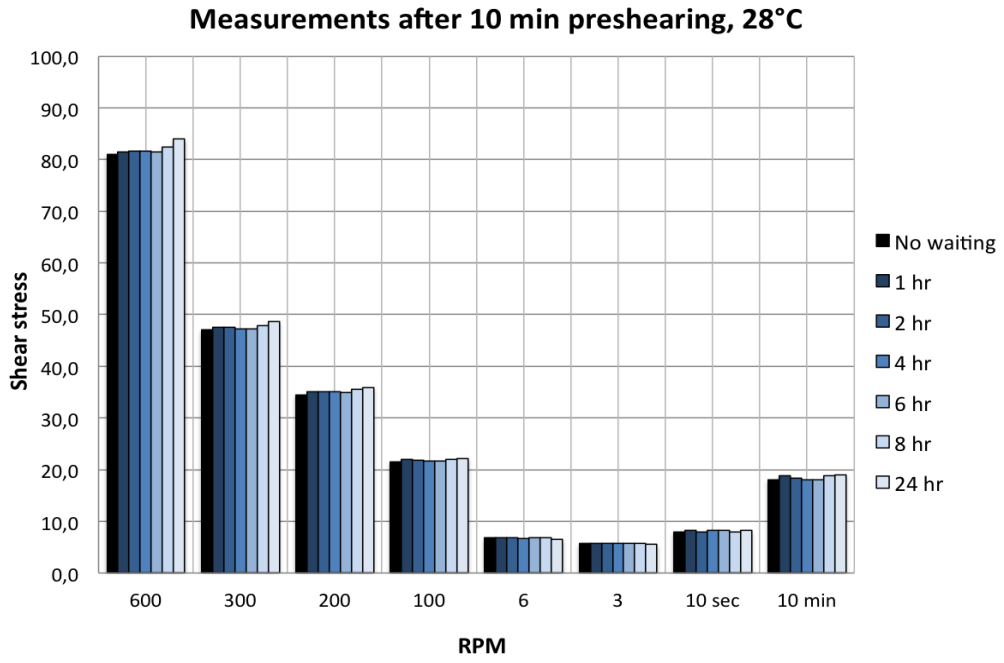

Figure 23: Fann 35 measurements on pre-sheared samples at 28 ºC

Fann 35 viscometer measurements at 50 °C:

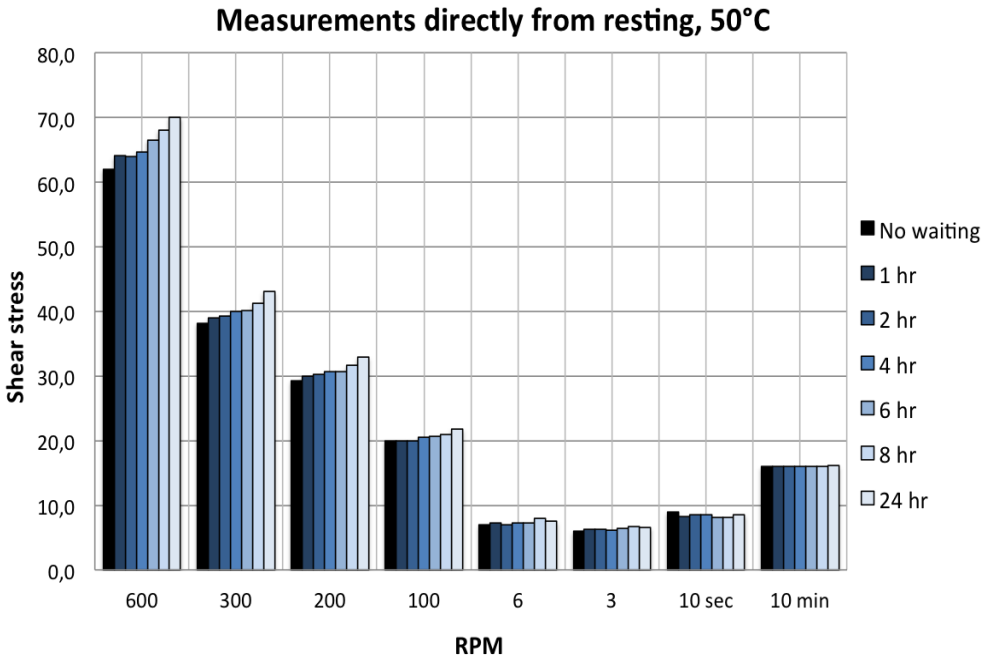

Figure 24: Fann 35 measurements on rested samples at 50 °C

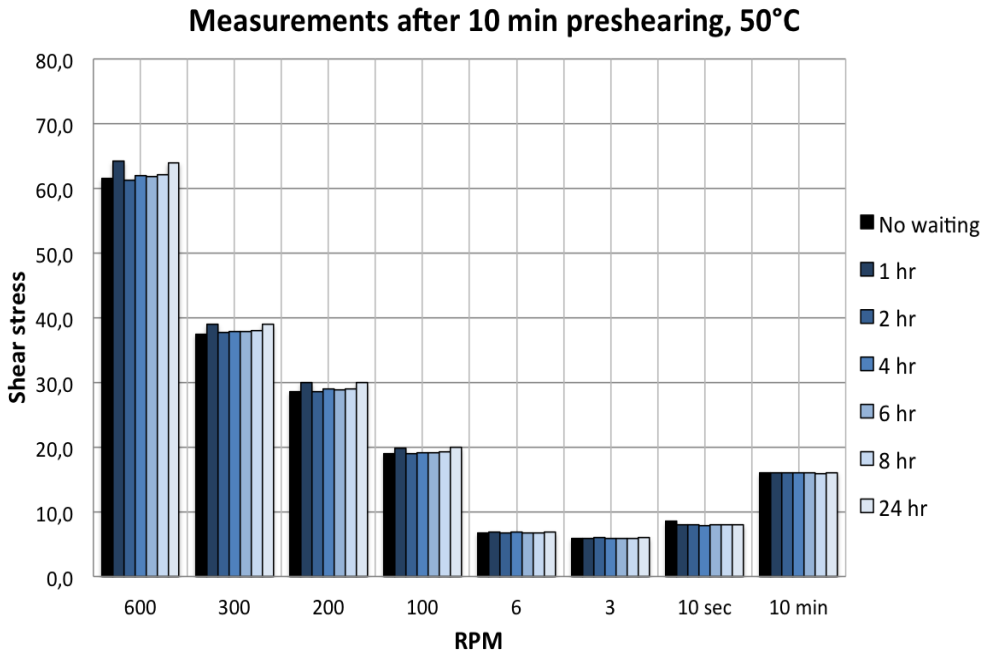

Figure 25: Fann 35 measurements on pre-sheared samples at 50 °C

Anton Paar Physica rheometer, Flow curve test:

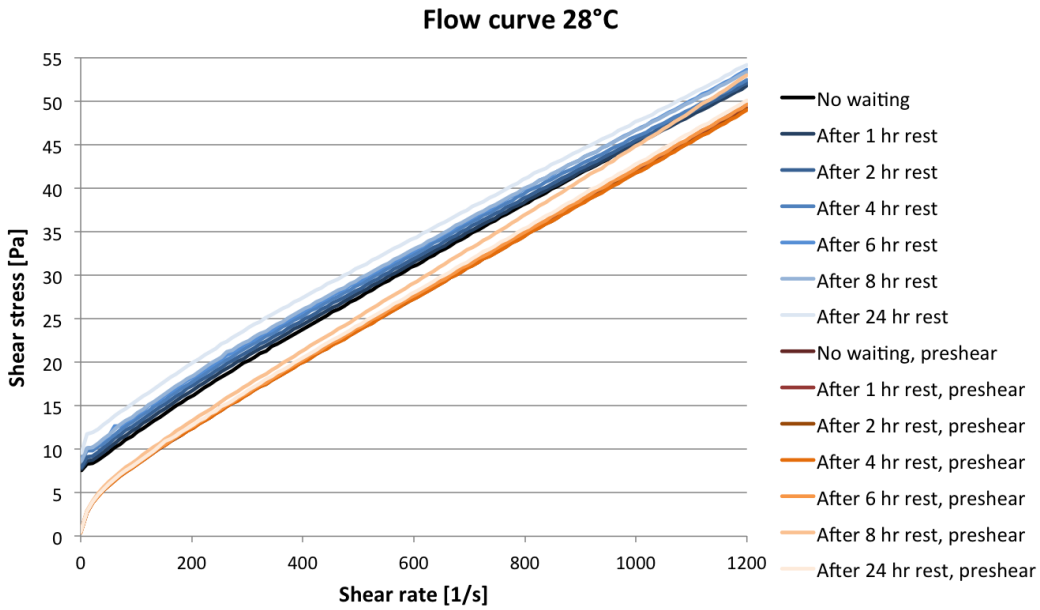

Figure 26: Anton Paar rheometer, flow curve measurements on rested and pre-sheared samples at 28 °C

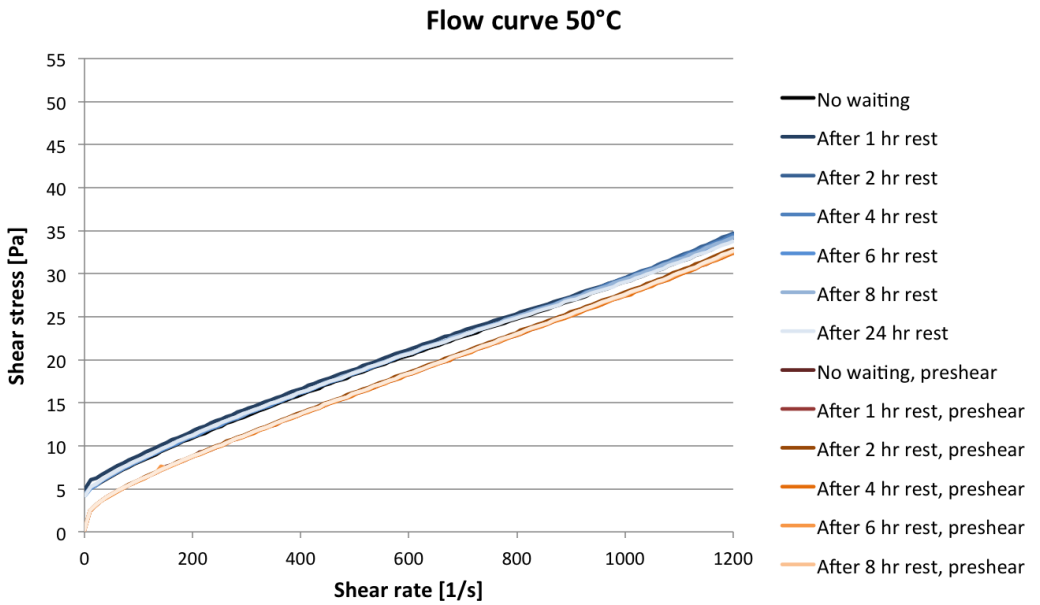

Figure 27: Anton Paar rheometer, flow curve measurements on rested and pre-sheared samples at 50 °C

Anton Paar Physica rheometer, Amplitude sweep test at 28 ºC:

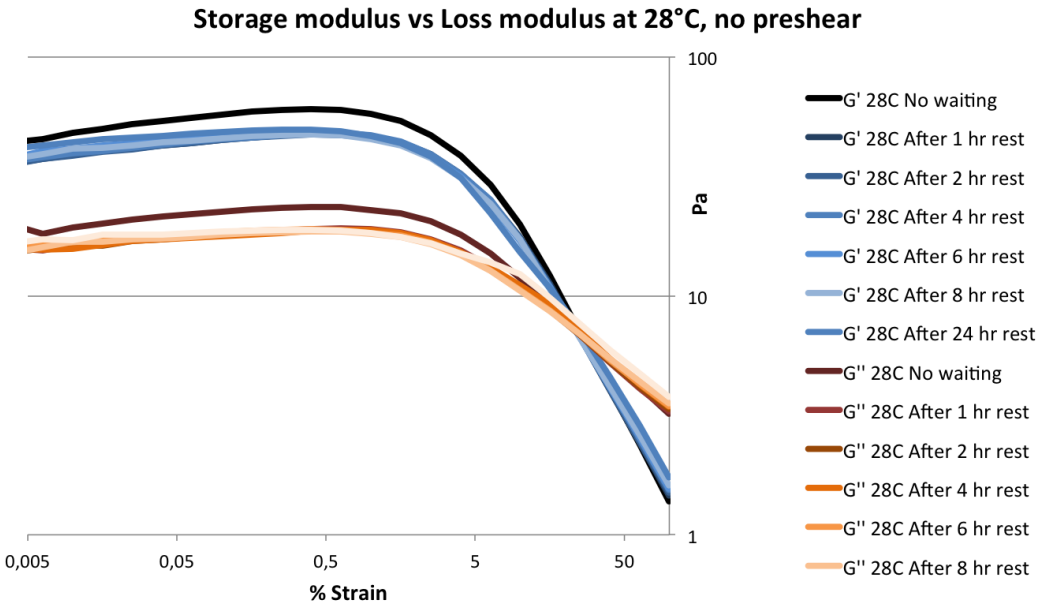

Figure 28: Anton Paar rheometer, storage modulus and loss modulus from Amplitude Sweep Test on rested samples at 28 ºC

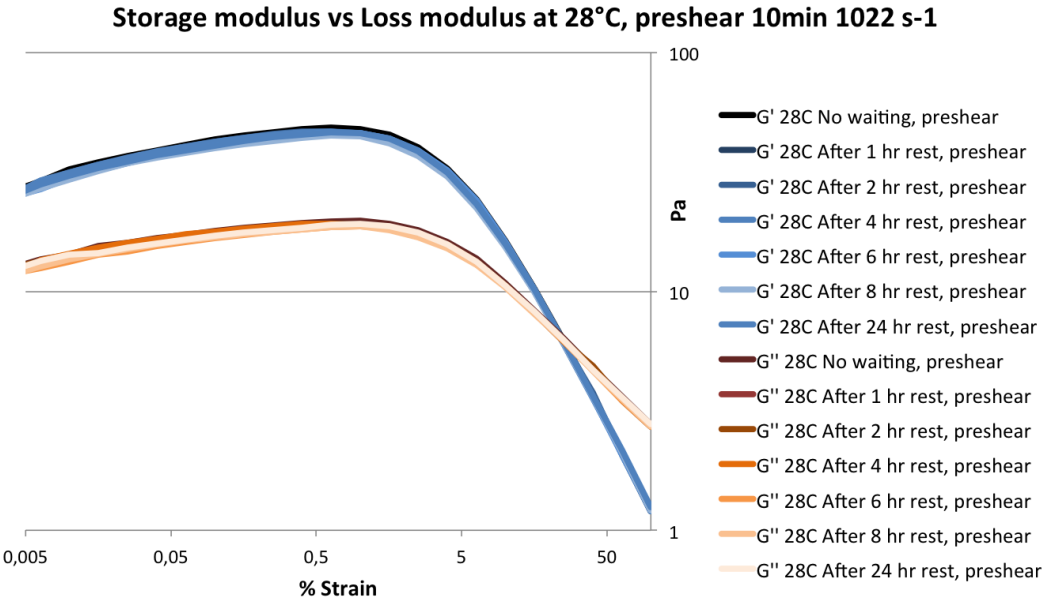

Figure 29: Anton Paar rheometer, storage modulus and loss modulus from Amplitude Sweep Test on pre-sheared samples at 28 ºC

Anton Paar Physica rheometer, Amplitude sweep test at 50 ºC:

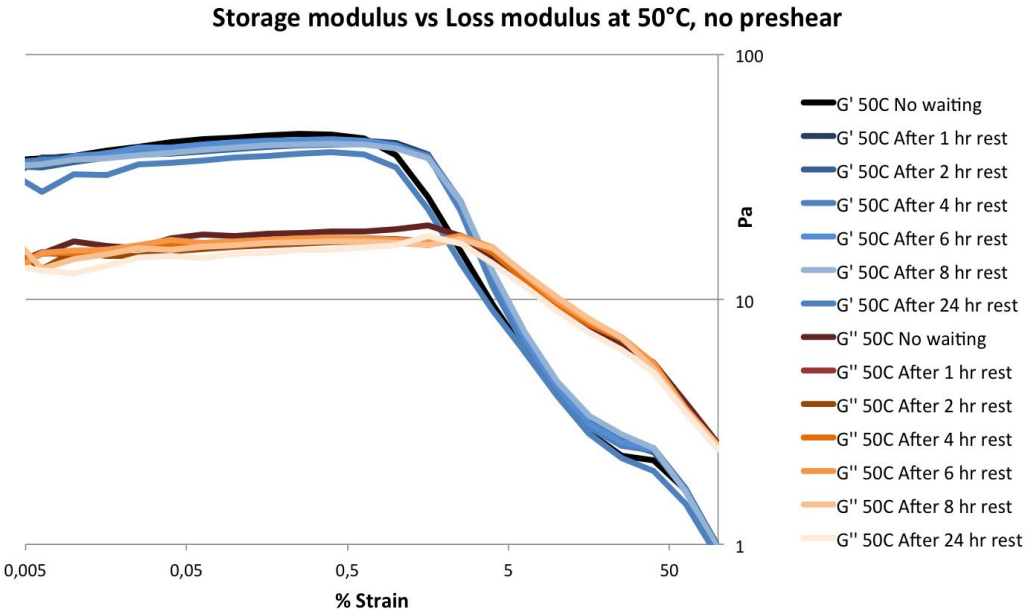

Figure 30: Anton Paar rheometer, storage modulus and loss modulus from Amplitude Sweep Test on rested samples at 50 ºC

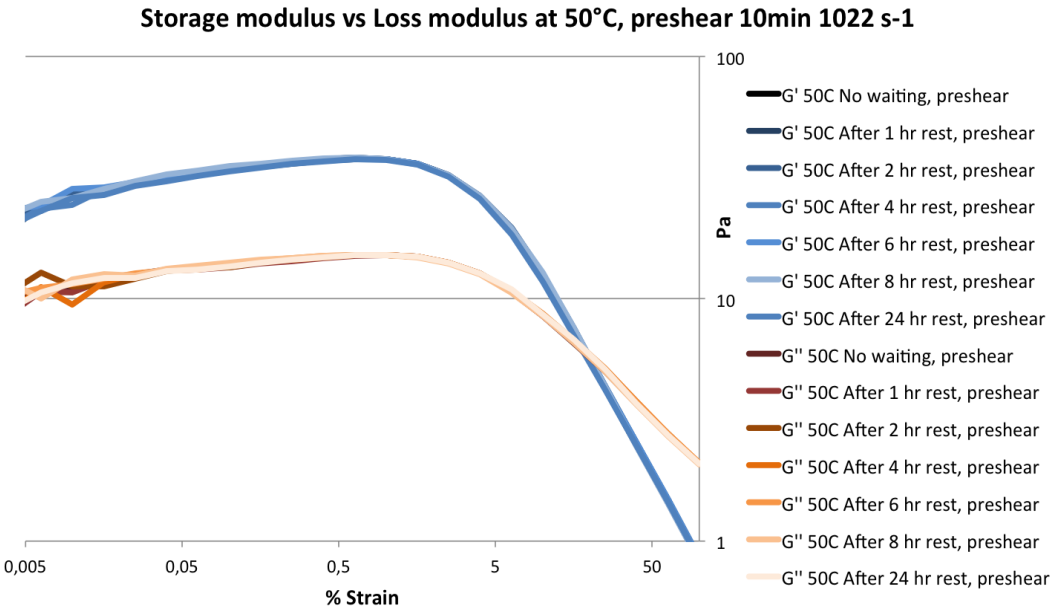

Figure 31: Anton Paar rheometer, storage modulus and loss modulus from Amplitude Sweep Test on pre-sheared samples at 50 ºC

4.3.2. Effect of evaporation in Anton Paar rheometer

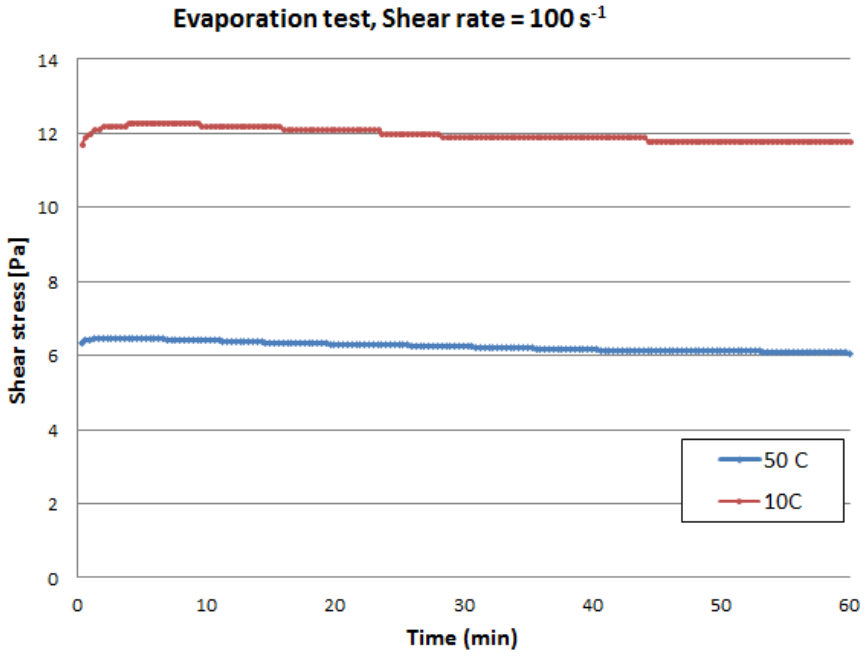

Figure 32: Evaporation test on OBM C with Anton Paar Physica rheometer

4.3.3. Effect of different fluid surface levels in the cup, Anton Paar Physica

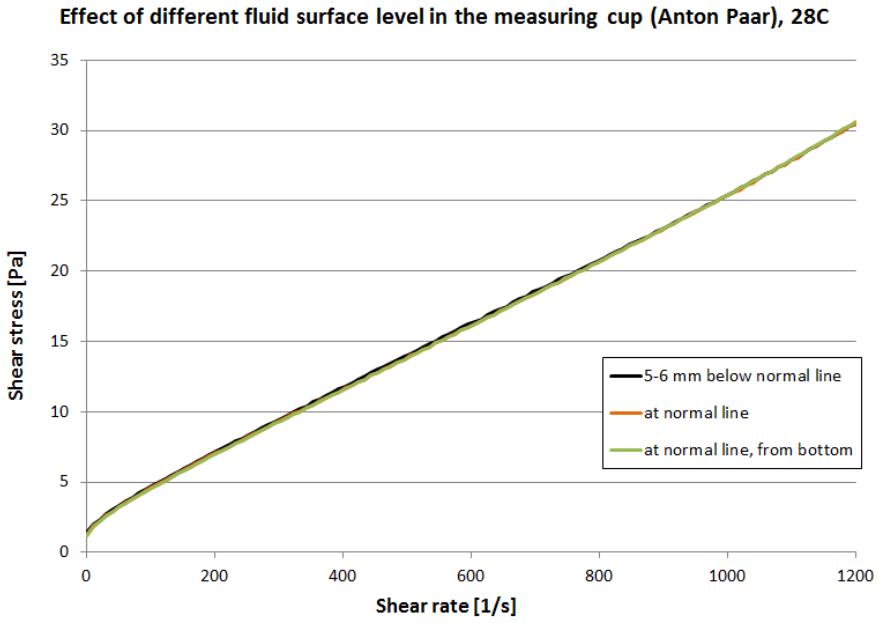

Figure 33: Flow curve test on OBM C with different surface levels in the cup

5. Evaluation of the results and discussion

5.1. Verification of rheological stability of the fluid in the flow loop

1) As mentioned in the results of Ch. 3.1., there was a problem with unstable rheology of OBM C, which was introduced into the flow loop in March. The viscosity profile of the fluid gradually decreased each week and more Bentone 128 (viscosifier) had to be added to the fluid in the flow loop in order to maintain the designed values.

   As a consequence of this, gel strength measurements were included into the test matrix in order to provide more information about the fluid condition. The ES measurements were intensified in this period as well, which became an essential part in finding out the reason of instability. The increase in the average value of Electrical Stability from 1402 V to 1999 V indicated that the oil-water ratio (OWR) of the drilling fluid OBM C was somehow influenced. A fluid sample was sent to M-I SWACO for measuring of the actual value of OWR. The test results showed that the OWR for OBM C was (95/5), while it was (84/16) for OBM B. As mentioned earlier, the composition of OBM C was as follows:

   - OBM C = OBM B + Bentone 128

   Since only solid material was added (Bentone 128), the OWR should not be influenced. This information, in addition to the fact that the viscosity profile of OBM C in the flow loop was gradually decreasing and more Bentone 128 had to be added into the system, lead the investigation to the conclusion that clay particles (Bentone 128) were reacting with the water in the emulsion and the product of reaction was gradually being filtered out from the system. This was confirmed by the inspection of the tank (Figure 34), which is attached to the sand filtering unit. It could be observed that also some free fluid had accumulated on top of the sand (due to gravity separation).

Figure 34: Tank for sand that is filtered out from the flow loop

2) Other data that are missing in the test results are the rheology measurements of OBM A at 50 ºC. The initial procedure of measuring included measurements only at 28 ºC, which was thought to be sufficient, since this was the ambient temperature in the set-up of the flow loop experimental rig. It was decided along the way that it would be more practical to do the measurements at 50 ºC in order to be able to compare the measured values directly with the values of initial design of the fluid system at M-I SWACO. From then, starting with OBM B, the measurements were performed both at 28 ºC and 50 ºC.

3) All the measurements were done directly after sampling the fluid from the active flow loop. A question was raised whether the shear rate in the experimental rig was sufficient enough to provide reproducible results and allow comparison of day-to-day measurements to track the changes in the rheology. A quick test was initiated. The viscosity profile of the sample was measured with Fann 35 viscometer. Directly after, a new sample from the same fluid batch was tested in similar way, but with a 5 min pre-shear at 600 rpm. The results did not indicate any changes in the viscosity profile. It was concluded that the fluid in the active

flow loop is sheared sufficiently enough to allow comparison of day-to-day measurements and that additional preconditioning of the samples was not necessary. Although this allowed tracking changes in the rheology of the fluids for this particular project, it is shown (Ch. 4) that preconditioning of samples is still necessary in qualitative research that goes beyond simple tracking of changes in rheology.

5.2. Evaluation of predicted pressure drop in the eccentric annulus

When working with wellbore stability in the field it is important to be able to predict the pressure losses in the wellbore. Some wells can be challenging and put a constraint in form of narrow pressure window. In such cases it is important that both the equivalent circulating density (ECD) and equivalent static density (ESD) do not exceed the limits of fracture pressure and pore pressure. Calculating the right pressure losses and in consequence designing a suitable fluid is vital to succeed. That is why one always tries to check or improve the theoretical models that already exist. In this section, we have validated the narrow slot approximation for estimation of pressure losses in eccentric annulus for HB-fluids and shown that the predictions match well with the experimental data, taken into consideration the following factors:

1) The Reynolds number used in the calculations was calculated by the narrow slot model approximation for concentric annuli. This is an additional error source. Ideally, a Reynolds number expression for eccentric annulus should be used. But Kelessidis et al. (2011) reported that there is no consensus among the research community on how one can define a non-ambiguous eccentric annulus Reynolds number.

2) One of the error sources in the quality of the experimental data on pressure drop in the annulus of the flow loop experimental rig is the temperature of the active fluid in the test section. From Tables 5-6, it can be seen that the inlet and outlet temperatures in the test section vary between 28 ºC - 31 ºC. The pressure drop that was estimated theoretically is based on the HB-parameters from the rheological measurements of the same fluid in Anton Paar rheometer. These measurements were performed at 28.0 ºC. The viscosity of a fluid depends highly on temperature and a change in temperature always will affect the viscosity. The temperature dependence is different for different

types of fluid. For some fluids a decrease of 1 ºC can cause a 10 % increase in viscosity (Mezger 2011). The temperature dependence can also be confirmed by the experiments of Politte (1985) on invert diesel oil emulsion mud, which is a good approximation for the OBM C fluid that was studied in this thesis.

3) Another source of error is the pressure offset that was measured for the DP4 cell (Figure 11). The experimental pressure drop values are not corrected for this offset. The drilling fluids that we have in the flow loop are non-Newtonian fluids with a yield stress. And it is assumed that the pressure offset is caused by this yield stress. To check this, the following calculations were performed:

The relationship between pressure offset and yield stress can be described as:

$$P_{\text{offset}} * A_{annulus} = Perimeter_{annulus} * \tau_{yield} \quad (27)$$

It can be observed in Figure 11 that the measured offset pressure for DP4-cell (4.2 m) is approximately 7 mbar. This corresponds to a pressure drop, given by:

$$dp/dx = P_{\text{offset}}/4.2m * 100\, Pa/mbar \quad (28)$$

Values for the annulus area of circular wellbore and perimeter of the annulus were taken from Appendix A:

$DP4$: P_{offset}	dp/dx	$A_{annulus}$	$Perimeter_{annulus}$	$\xrightarrow{yields}$	τ_{yield}
[mbar]	[Pa/m]	[m^2]	[m]		[Pa]
7	167	0.005891	0.314		3.13

The yield stress for OBM C that was used in Herschel-Bulkley model fitting, as depicted in Figure 13, is 2.84 Pa. The value that is calculated above deviated a little from this value, but within the limits of uncertainty. As it was described by Sandvold (2012), the yield stress value depends strongly on the method, by which it was measured. Small variations can occur for different methods used on the same fluid.

4) Observing the estimated pressure drop values in Figure 14 and Figure 15, it can be seen that these are lower for eccentric annulus than for concentric annulus. This is not a coincidence and this pressure drop reduction in eccentric annuli can be confirmed by Silva and Shah (2000), who concluded that the friction pressure losses in fully eccentric annulus were found to be on average 18 to 40 % lower than in concentric annulus, and that these losses were independent of the fluid type and the flow regime. Kelessidis et al. (2011) also reported that a 100 % eccentric annulus presents pressure loss data that range between 55 % and 70 % of the concentric case.

5) Surface roughness was not considered in the calculations of pressure drop estimation. The annulus was considered smooth with a very small wall roughness, probably introducing a small error. This factor is expected to have even smaller effect in the laminar flow, as in our case. One would expect that surface roughness will increase pressure drop in the annulus, the magnitude of which should be evaluated both experimentally and theoretically, but none of the available models takes it into account, neither for concentric nor for eccentric annuli (Kelessidis et al. 2011).

6) The eccentricity correction factor of Haciislamoglu et al. (1990), used in the calculations is valid for the eccentricities up to 0.95. In the calculations, 1.0 eccentricity was used, introducing thus an error. Additionally, the Haciislamoglu correlation itself has an accuracy of +/- 5%.

7) When calculating the Reynolds number for the lower limit of transitional region of flow Eq.24 was used. Normal flow index value n was used instead of the local value of flow index, n', which is defined as:

$$n' = \frac{n(1-\xi)(n\xi+\xi+1)}{1+n+2n\xi+2n^2\xi^2} \tag{29}$$

Considering the purpose of the calculation; finding the lower limit of Re where the transitional flow starts, this was considered a good enough approximation.

5.3. Evaluation of the methodology study results

The effect of resting time and pre-shear on rheology

Figures 22-25 show viscosity profiles for OBM C, measured with Fann 35 viscometer at both 28 ºC and 50 ºC. It can be observed that the readings were higher for the rested samples than for the pre-sheared samples. It shows that there is colloidal structure development ongoing with time, calculated to be around 2-9% when the samples are not subject to shear. For the pre-sheared samples we can observe lower and flatter readings, with 1-3% increase with time. It is concluded that the pre-sheared samples give more reproducible results at both temperatures, except for 24 hr measurements. Even with pre-shearing, sample readings change after 24 hours for measurements at 50 ºC and after 8 hours for measurements at 28 ºC.

Fluid batches that were used for the Anton Paar rheometer experiments on the effect of resting/pre-shearing, were preliminarily sheared for 10 minutes at approximately 13000 rpm, as described in Ch. 4.1.3. This was done in order to have identical fluid conditions for the different days, since the experiments took 5 days.

In Figure 26, we can observe that with no pre-shear, the structure regenerates (after shearing at 13000 rpm) measurably with time, for 28 ºC. The structure regeneration is much less pronounced for flow curve measurements at 50 ºC (Figure 27). By comparing the flow curves for the different temperatures, it can be observed that pre-shearing has less effect at 50 ºC.

Figures 28-31 show that the pre-sheared samples give more reproducible amplitude sweep results. It can also be seen that the measurements at 50 ºC are more sensitive to pre-shear.

Below, some comments on the relevant error sources are listed:

1) For Fann 35 viscometer, a thermocup was used for heating of the samples to the right temperatures. The temperature was controlled by a rotary switch that only increased or decreased the level of heating and did not allow setting a constant temperature value. This posed a little challenge and some time was spent to learn

how to adjust this rotary switch to reach the temperatures of 28 ºC and 50 ºC. In addition, the heat was distributed from the walls of the thermocup and rotation had to be applied to distribute it further through the sample in the cup. The rotation posed another challenge since half of our measurements were on samples that were rested, and external forces would break the colloidal structure and decrease the reading values. The rotation was diminished to the minimal amount, seldom exceeding 30 sec in total. Still, the effect of resting was reduced. (Some samples took 20 sec to confirm the right temperature and some took more than 30 sec. This is the reason to why the "1hr"-measurements are higher than the "2hr"-measurements at 28 ºC rested fluid).

All of these challenges were even bigger for the 10 min gel measurements, because the fluid could neither be stressed by the temperature indicator stick or rotation applied for distribution of the temperature. By trial and error method the procedure was mastered to an acceptable level. The temperatures were measured both before the first measurement, before the 10 sec gel measurement and after the 10 min gel measurement to document that it was within the limits of acceptable deviation. For all the measurements the temperature accuracy was within 0.5 ºC.

For the 10 min gel measurement, it was observed that the temperature in the middle of the cup (farthest distance from the heated walls) was few degrees below the outer wall temperature. To counter that, a higher temperature was set for the 10 min gel measurements. In the solution, the temperature in the middle of the cup was around 48.5 ºC, while at the walls it was kept at around 51.5 ºC.

In spite of all of the aforementioned challenges the measuring procedure was exactly the same for all the measurements. Any potential error sources were identical for all of the measurements. Thus allowing us to demonstrate the tendencies clear enough.

2) "1hr"-measurements on pre-sheared samples at 50 ºC is higher than the others (Figure 25). No particular reason was observed. All the other measurements follow the pattern. The same goes to the "8hr"-measurement of flow curve on pre-sheared samples (Figure 26).

3) The readings from Fann 35 viscometer were called “shear stress” without specifying the unit, which is centiPoise. These readings were not used in any calculations; hence, specification of the unit was omitted. The diagrams in Figures 22-25 show the tendencies of the effect of resting/pre-shearing clear enough for drawing conclusions.

The effect of evaporation, Anton Paar rheometer

It was not possible to detect whether evaporation affects the measurements in Anton Paar rheometer due to the shear-thinning property of the tested fluid (OBM B).

1) Initially, the experiment was performed only at 50 ºC, since only at this temperature sufficient evaporation could be expected to happen. As can be seen in Figure 32, the readings gradually decrease. It was not clear, whether this was an effect of evaporation or an effect of shear-thinning. To find answer, the experiment was repeated at 10 ºC. The same pattern could be observed at this temperature. It was concluded that the gradual decrease in readings was due to the shear-thinning effect of the tested fluid. The effect of evaporation could not be documented with this fluid. Nor can it be detected with any other oil-based drilling fluid with shear-thinning property.

2) An increase in the readings can be observed during the first 2 minutes of the test. The reason is that the sample was pre-sheared for 10 minutes at 1000 s^{-1}. The microstructure was broken due to the effect of strain deformation, and it slowly builds up again under low shear rate (Maxey et al. 2008; Bui et al. 2012).

3) It is interesting to observe that the microstructure regenerates and gives higher readings of viscosity (in the beginning), which then fall again under the same shear rate. The experiment was also performed without pre-shearing in order to exclude the effect of structure regeneration. This experiment (Figure 35) showed the same declining curve, now without the increase in the readings in the beginning. It was still not possible to conclude how much of this decline was due to evaporation. One possible way to solve this could be to exclude the effect of evaporation by conducting this experiment in a closed system (another model of

concentric cylinder in Figure 19), leaving only the shear-thinning effect. If we then observed the same decline in readings, we could conclude that it was due to the shear-thinning. This was not done, because there was no suitable equipment.

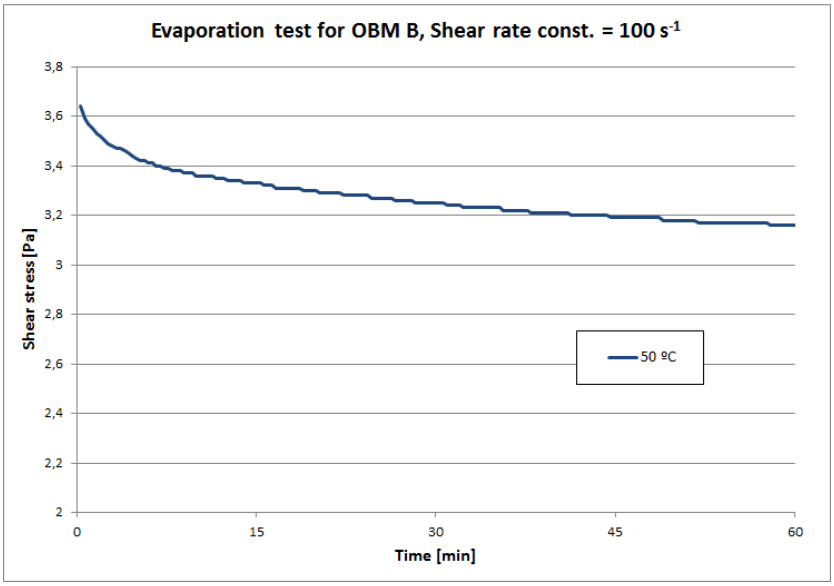

Figure 35: Evaporation test without pre-shearing, OBM B

4) Another possible way to detect the evaporation was to measure densities before and after the experiment at 50 ºC. If we then observed that the density increased, it could indicate that the lighter particles in the sample had evaporated, as expected. The evaporation experiment was repeated by SINTEF in Bergen, where they had a more precise density measuring tool (Anton Paar densitometer). The densities of the sample were measured before and after the 50 ºC measurement:

Before:	1.254 g/cm^3 (at 20 ºC)
After:	1.239 g/cm^3 (at 20 ºC)
Decrease:	1.20%

The results showed that the density decreased by 1.20 % after 1 hour at 50 ºC, which did not indicate any effect of evaporation.

The effect of different fluid surface levels in the cup, Anton Paar rheometer

As can be seen from the results of 3 measurements in Figure 33, a deviation of 5-6 mm in fluid surface level of samples in the measuring cup did not affect the measurements.

1) The reason behind choosing exactly 5-6 mm was the conclusion that one never exceeds this limit of human error in sample preparation.

2) The added 5-6 mm of fluid in the "normal line"-test was taken with a pipette from the top of the fluid batch used for the experiment. No change in measurements was observed, compared with the "5-6 mm below normal line"-test, meaning that the rotating bob was exposed to the same amount of stress. It was suspected that the added 5-6 mm from the top of the fluid batch contained only lighter particles, while the heavier particles (barite) sagged to the bottom (Saasen 2002). The "normal-line"-test was repeated after removing 5-6 mm of fluid from top of the cup and replacing this with new 5-6 mm from bottom of the fluid batch.

3) The 5-6 mm added/removed were measured by eye, which represents an error source. But for the purpose of the experiment this was sufficient, and the conclusion drawn from the results were regarded as acceptable.

6. Self-assessment

The method for estimation of pressure losses in eccentric annulus that was derived in Ch.3.2. matched well with the experimental data for two different fluid systems, OBM B and OBM C. The narrow slot approximation method that was applied proved to be good in estimating the pressure drop, when corrected with the Haciislamoglu correction factor for eccentricity. It was not possible to estimate, how much of the error was from the correction factor and how much was from the narrow slot approximation. A way to check this could be to compare the estimation for concentric annulus (before correcting for eccentricity) with real data from concentric annulus. But these data were missing for the OBM B and OBM C since the set-up of the drill string in the experimental rig was eccentric.

One may as well wonder how well the method estimates pressure losses for other types of Herschel-Bulkley (HB) fluids, for instance water-based drilling fluids (WBDF). Pressure data from earlier experiments on WBDF were available, but the fluids were no longer present and the HB model parameters could not be determined.

Taking into consideration all of the error sources that were listed in Ch. 5.2., it is understandable that the estimation can never fully match the real data. Even if we diminish the error sources to the minimal, the calculation is still based on approximations. Hence, it can be concluded that the derived estimation method is a good enough approximation for laminar flow conditions, which prevailed in the experimental rig for all the given flow velocities. In the future, the equations could be extended to include transitional and turbulent flow regimes. But first, the experimental rig must be adjusted to allow conducting experiments at higher flow rates.

Regarding the study on evaluation of quality and methodology of rheological measurements, the results from the experiments on resting/pre-shearing effects are to be published in the Annual Transactions of the Nordic Rheology Society (vol. 23, 2015), and may serve as a methodical reference work and a practical guide. In this study, the effects of resting/pre-shearing were quantified for both simple viscosity

measurements (direct-reading viscometer) and for measurements of viscoelastic properties (rheometer). The error sources were listed in Ch.5.3.

It was concluded that for comparative data, pre-shearing was recommended to get more reproducible results. This is valid for viscosity profile measurements with both direct-reading viscometers and more complex rheometers. But it should be noted that for in-depth characterization of rheological properties, such as linear viscoelastic region, cross-over point (Assembayev et al. 2015) and yield stress, pre-shearing should be thoroughly considered as viscoelastic properties are affected by pre-shear.

The experiment on evaporation effect on measurements did not lead to any clear indications of evaporation. Several methods were applied without giving any results. It could be suggested to perform the experiment in a closed system, as described in Ch. 5.3. This would tell something about how big the effect of evaporation is, but still not quantify the effect.

7. Conclusion

By using a real oil-based drilling fluid and an experimental rig that closely simulates real well conditions, the following conclusions were made:

- Herschel-Bulkley rheology model is shown to be the model that fits best the rheology of the oil-based drilling fluids used in our experiments.
- The narrow slot approximation derived for concentric annulus and used together with the Haciislamoglu eccentricity correction factor gives good predictions of pressure drop in eccentric annulus for non-rotating string and no sand injection.

A study was conducted on the quality of the rheological measurements and the methodology used for performing these, with following conclusions:

- The colloidal structure of fluids strengthens with time when not subject to shear. This behaviour influences the viscosity measurements.
- For comparative data, pre-shearing is recommended to get more reproducible results.

The results from the study on resting/pre-shearing effects were submitted and accepted in a paper for the Annual Transactions of the Nordic Rheology Society (vol. 23, 2015), and may serve as a methodical reference work and a practical guide.

Abbreviations and symbols

Abbreviations

API	American Petroleum Institute
DP	differential pressure
ECD	equivalent circulating density
ES	electrical stability
ESD	equivalent static density
HB	Herschel-Bulkley
IADC	International Association of Drilling Contractors
ID	inner diameter
LVER	linear viscoelastic range
OBDF	oil-based drilling fluid
OBM	oil-based mud
OD	outer diameter
OWR	oil water ratio
RPM	revolutions per minute
SPE	Society of Petroleum Engineers
SG	specific gravity
vs.	versus
Re	Reynold's number

Symbols

dp/dx	Pa/m	Pressure gradient
e		Eccentricity
n		Flow behaviour index
t	sec ; hr	Time
A	m^2	Area
D_h	m	Hydraulic diameter
D_i	m	Inner diameter
D_o	m	Outer diameter
F	N	Force
G'	Pa	Shear storage modulus
G''	Pa	Shear loss modulus
K	$Pa * s^n$	Consistency index
P	Pa	Pressure
R		Haciislamoglu correction factor
U	m/s	Flow velocity

$\dot{\gamma}$	s^{-1}	shear rate
δ	m	annular gap for a concentric annulus
μ	Pas	viscosity
μ_{eff}	Pas	effective viscosity
μ_{pl}	Pas	plastic viscosity
ξ		Dimensionless shear rate
ρ	kg/m^3	Density
τ	Pa	Shear stress
τ_w	Pa	wall shear stress
τ_y	Pa	yield point (yield stress)

List of figures

List of tables

References

Aadnoy, B.S. , Cooper, I. , Miska, S. et al. 2009. *Advanced drilling and well technology*, first edition. Richardson, TX: Society of Petroleum Engineers.

Anton-Paar 2015. *Anton Paar MCR302 rheometer* http://www.anton-paar.com/se-en/products/details/mcr-rheometer-series/rheometer/ (accessed 26 May 2015)

API RP 13B-2, *Recommended practice for field testing oil-based drilling fluids*, *Ch.7.3*, 2008. Washington, DC: API.

API RP 13I, *Recommended practice for laboratory testing of drilling fluids*, *Ch. 26.4*, eighth edition, 2009. Washington DC: API.

Assembayev, D. , Myrseth, V. , Werner, B. et al. 2015. Establishing an experimental pre-conditioning procedure for rheological characterization of oil based drilling fluids. *Annular transactions of the Nordic rheology society* **23**.

Bui, B. , Saasen, A. , Maxey, J. et al. 2012. Viscoelastic properties of oil-based drilling fluids. *Annular transactions of the Nordic rheology society* **20**.

Brent, R. P. 1973. *Algorithms for Minimization without Derivatives, Chapter 3-4.* Englewood Cliffs, New Jersey: Prentice-Hall.

Buchtelova, M. 1988. Comments on "The axial laminar flow of yield-pseudoplastic fluids in a concentric annulus". Ind. Eng. Chem. Res., **27**(8): 1557-1558. http://dx.doi.org/10.1021/ie00080a040.

Cengel, Y.A. and Cimbala, J.M. 2006. *Fluid Mechanics (SI Units): Fundamentals and Applications,* 2nd revised edition. McGraw-Hill Professional.

Clark, R. 2015. *Understanding Rheology. San Diego R&D*, uow.edu.au, 17 July 2011, http://www.uow.edu.au/content/groups/public/@web/@sci/@chem/documents/doc/uow107427.pdf (accessed 5 May 2015)

Dodge, D.W. and Metzner, A.B. 1959. Turbulent flow in non-Newtonian systems. *Aiche Journal* **5** (2): 189-204. http://dx.doi.org/10.1002/aic.690050214

Drillingformulas.com. 2012. Flow Regime and Critical Reynolds Number for Drilling Hydraulics, 7 May 2012, http://www.drillingformulas.com/flow-regime-and-critical-reynolds-number-for-drilling-hydraulics (accessed 25 April 2015).

Etcy 2015. Hamilton Beach Scovill mixer, www.etsy.com/listing/192234987/hamilton-beach-scovill-milkshake-maker (accessed 26 May 2015)

Fordham, E.J. , Bittleston, S.H. and Tehrani, M.A. 1991. Viscoplastic flow in centered annuli, pipes and slots. Ind. Eng. Chem. Res., 30(3): 517-524. http://dx.doi.org/10.1021/ie00051a012.

Forsythe, G.E. , Malcolm, M.A. and Moler, C.B. 1977. *Computer methods for mathematical computations, Ch. 7,* first edition. Englewood Cliffs, New Jersey: Prentice Hall.

Founargiotakis, K. , Kelessidis, V.C. and Maglione, R. 2008. Laminar, transitional and turbulent flow of Herschel-Bulkley fluids in concentric annulus. *Can J Chem Eng* **86** (4): 676-683. http://dx.doi.org/10.1002/cjce.20074.

Guillot, D. 1990. Rheology and flow of well cement slurries. In Nelson, E. and Guillot, D. (eds) *Well Cementing,* Schlumberger. Sugar Land, Texas, 2006, Chapter 4.

Haciislamoglu, M. and Cartalos, U. 1994. Practical pressure loss predictions in realistic annular geometries. Presented at the SPE Annual Technical Conference and Exhibition, New Orleans, Louisiana, 25-28 September, SPE-28304-MS. http://dx.doi.org/10.2118/28304-MS

Haciislamoglu, M. and Langlinais, J. 1990. Non-Newtonian flow in eccentric annuli. *J Energy Resour Technol* **112** (3): 163-169. http://dx.doi.org/10.1115/1.2905753

Hanks, R. W. 1979. The axial laminar flow of yield-pseudoplastic fluids in a concentric annulus. Ind. Eng. Chem. Proc. Des. Dev., **18** (3):488-493. http://dx.doi.org/10.1021/i260071a0024

Hansen, S.A., Rommetveit, R., Sterri, N. et al. 1999. A new hydraulics model for slim hole drilling applications. Presented at the SPE/IADC Middle East Drilling Technology Conference, Abu Dhabi, UAE, 8-10 November, SPE-57579-MS. http://dx.doi.org/10.2118/57579-MS.

Kelessidis, V.C., Maglione, R., Tsamantaki, C. et al. 2006. Optimal determination of rheological parameters for Herschel-Bulkley drilling fluids and impact on pressure drop, velocity profiles and penetration rates during drilling. *J Pet Sci Eng* **53** (3): 203-224. http://dx.doi.org/10.1016/j.petrol.2006.06.004

Kelessidis, V.C., Dalamarinis, P., and Maglione, R. 2011. Experimental study and predictions of pressure losses of fluids modeled as Herschel-Bulkley in concentric and eccentric annuli in laminar, transitional and turbulent flows. *J Pet Sci Eng* **77** (3):305-312. http://dx.doi.org/10.1016/j.petrol.2011.04.004

Langlinais, J.P. , Holden, W.R. and Bourgoyne, A.T. 1983. Frictional pressure losses for the flow of drilling mud and mud/gas mixtures. SPE Annual Technical Conference and Exhibition, San Francisco, California, 5-8 October, SPE-11993-MS. http://dx.doi.org/10.2118/11993-MS.

Lund, B. 2014. Memo-note on "Pressure loss in concentric annuli for Herschel-Bulkley fluids".

Lund, B., Ytrehus, J.D., Taghipour, A. et al. 2015. Oil based drilling fluids in circular wellbore, horizontal and inclined. Presented at internal SINTEF meeting, May 2015.

Maxey, J. , Ewoldt, R. , Winter, P. et al. 2008. Yield stress: what is the "true" value? Presented at the AADE Fluids Conference and Exhibition, Houston, Texas, April 8-9, 2008, AADE-08-DF-HO-27.

Mezger, T.G. 2011. *The Rheology Handbook: For users of rotational and oscillatory rheometers,* 3rd revised edition. Vincentz Network.

Ofi Testing Equipment 2014, Catalogue of products. http://www.ofite.com/products/product/482-emulsion-stability-tester (accessed 25 May 2015)

Okafor, M.N. and Evers, J.F. 1992. Experimental comparison of rheology models for drilling fluids. Presented at the SPE Western Regional Meeting, Bakersfield, California, 30 March-1 April, SPE-24086-MS. http://dx.doi.org/10.2118/24086-MS

Petrowiki. 2015. Oil emulsions (25 March 2015 revision), www.petrowiki.org/Oil_emulsions (accessed 5 May 2015).

Pilehvari, A. and Serth, R. 2009. Generalized hydraulic calculation method for axial flow of non-Newtonian fluids in eccentric annuli. *SPE Drill & Compl* **24** (04): 553-563. SPE-111514 PA http://dx.doi.org/10.2118/111514-PA.

Politte, M.D. 1985. Invert oil mud rheology as a function of temperature and pressure . Presented at the SPE/IADC 1985 Drilling Conference, New Orleans, Louisiana, March 5-8, 1985, SPE-13458-MS http://dx.doi.org/10.2118/13458-MS.

Reed, T.D. and Pilehvari, A.A. 1993. A new model for laminar, transitional and turbulent flow of drilling muds. Presented at the SPE Production Operations Symposium, Oklahoma City, Oklahoma, 21-23 March, SPE-25456-MS.
http://dx.doi.org/10.2118/25456.MS

Saasen, A. 2002. Sag of weight materials in oil based drilling fluids. *Proc.*, IADC/SPE Asia Pacific Drilling Technology, Jakarta, Indonesia, 8-11 Septermber, SPE-77910-MS.
http://dx.doi.org/10.2118/77190-MS

Sandvold, I. 2012. *Gel evolution in oil based drilling fluids*. MS thesis, Norwegian University of Science and Technology, Trondheim (June 2012).

Schlumberger 2015. Fann viscometer, http://www.glossary.oilfield.slb.com/en/Terms/f/fann_viscometer.aspx (accessed 10 May 2015)

Silva, M.A. and Shah, S.N. 2000. Friction pressure correlations of Newtonian and non-Newtonian fluids through concentric and eccentric annuli. SPE/ICoTA Coiled Tubing Roundtable, Houston, Texas, 5-6 April, SPE-60720-MS.
http://dx.doi.org/10.2118/60720-MS

Taghipour, M.A. 2014. *Hole cleaning and mechanical fricition in non-circular wellbore geometry*. Doctoral thesis, Norwegian University of Science and Technology (June 2014). 2014:88

UiS. 2011. *Øvinger i Bore- og Brønnvæsker*. Universitetet i Stavanger.

Werner, B. 2014. *Investigation of Drilling Fluid Performance*. BSc thesis, Montanuniversitat Leoben, Leoben (March 2014)

Ytrehus, J.D. , Taghipour, A. , Lund, B. et al. 2014. Experimental study pf cuttings transport efficiency of water based drilling fluids. Proc., ASME 2014 33rd International Conference on Ocean, Offshore and Arctic Engineering, Vol. **5**. San Francisco, California, June 8-13, 2014. OMAE2014-23960.
http://dx.doi.org/10.1115/OMAE2014-23960.

Appendices

Appendix A - Key parameters of the test section in the experimental rig

Description	Value
Total length from inlet to outlet	10 m
Distance between measuring points for instrument DP2	4,2 m
Distance between measuring points for instrument DP3	1 m
Diameter of circular wellbore	100 mm
Drift diameter of non-circular wellbore	100 mm
Total inner area of circular wellbore	7850 mm^2
Total inner area of non-circular wellbore	10167 mm^2
Outer diameter of inner pipe	50 mm
Annular flow area of circular wellbore	5891 mm^2
Annular flow area of non-circular wellbore	8204 mm^2
Perimeter length of circular wellbore	314 mm
Perimeter length of non-circular wellbore	379 mm
Mass per unit length of inner pipe, seasons 3&4	8.75 kg/m
Inclination of wellbore from vertical	0° and 60°

Table 8: Specifications of the test section, updated April 2015.

Annular velocity (m/s)	Flow rate (l/min)	
	Circular geometry	Non-circular geometry
0.54	190.5	265.8
0.75	265	369.4
1.04	369	514
1.45	513.5	715.5

Table 9: Flow velocities and flow rates in the flow loop experimental rig.

Appendix B – Verification data of the rheological stability in the flow loop

Few measurements were taken during February due to problems with the flow loop.

Date	Fluid/ Fluid history	Fluid name	T [C]	rpm							Gel strength		Comment
				3	6	100	200	300	600	10 sec	10 min	
21.jan.15	Versatec 1,28 + 800L Base oil	OBDF A	28	2,5	3	9	14,5	19,5	35			New density due to weight material loss Density 1,11sg
23.jan.15	Versatec 1,28 + 800L Base oil	OBDF A	28	3	3,5	11	17	23	39			
26.jan.15	Versatec 1,28 + 800L Base oil	OBDF A	28	3	4	11	17	22,5	40			Emulsion stability (ES) 784 V
26.jan.15	Versatec 1,28 + 800L Base oil	OBDF A	28	3	4	11	17	23	39			
27.jan.15	Versatec 1,28 + 800L Base oil	OBDF A	28	3	3,5	11	17	23	40			
27.jan.15	Versatec 1,28 + 800L Base oil	OBDF A	28	3,5	4	11,5	17	23	40			
28.jan.15	Versatec 1,28 + 800L Base oil	OBDF A	28	3	3,5	11	17	23	40			
02.feb.15	Versatec 1,28 + 800L Base oil	OBDF A	28	3	3,5	11	17	22	39			
04.feb.15	Versatec 1,26, weighted w/200L Versatec 1,5	OBDF B	28	4	4,5	16	25	33	58			
05.feb.15	Versatec 1,26, weighted w/200L Versatec 1,5	OBDF B	28	4	4,5	15	24	32,5	57			
04.feb.15		OBDF C	28	5	6	17,5	27	36	61			
06.mar.15		OBDF B	28	3	4	13,5	21,5	29	50			
06.mar.15	Same sample as from the 4th of March	OBDF C	28	5,5	6	20	31	41	67			Sample was mixed in Waring blender prior to measurement
			50	5	5,5	15	22	27	43			
06.mar.15		OBDF C	28	5	6	18,5	29	38	63			Bentone 128 added stepwise, higher concentration, 13,7g/l
10.mar.15	Sample before addition of Bentone 128	OBDF B	**28**	3	3,5	11,5	18	25	44			
			50	2,5	3	8	12,3	17	28	6	6	ES 870V
10.mar.15		OBDF C	**50**	8	9	20	28	37	58			
10.mar.15		OBDF B	**50**	4	5	12	17,5	22	35			
10.mar.15		OBDF B	**28**	5	5,5	15,5	25	34	59			
12.mar.15		OBDF C	**50**	6,5	7,5	19	28	36	59	8	12 (1 min)	
13.mar.15		OBDF C	**50**	6	7	18	26,5	35	57	8,5	11 (1 min)	
16.mar.15		OBDF C	**50**	6	7	18	26,5	35	56	8,5	11 (1 min)	
17.mar.15		OBDF C	**28**	7	8	24	38	51	85			
17.mar.15		OBDF C	**50**	6	7	18	27	35	57	7	9	ES 1402 V
18.mar.15		OBDF C	**28**	7	8	25	39,5	54	90	10	17 (5 min)	
18.mar.15		OBDF C	**50**	6,5	7	18	26	34	55	8	12,5 (5 min)	
19.mar.15	Adjusted viscosity in a sample with 2 g/l Bentone	OBDF C	**50**	5,5	6	16,5	25	33	54	7	9 (1 min)	
			50	6	7	19,5	30	39	63	8,5	11 (1 min)	

Table 10: Rheology measurements of the fluid in the flow loop, January-March 2015.

Table 11: Rheology measurements of the fluid in the flow loop, March-April 2015.

Date	Fluid/ Fluid history	Fluid name	T [C]	rpm						Gel strength		Comment
				3	6	100	200	300	600	10 sec	10 min	
20.mar.15		OBDF C	28	6,5	7,5	24	39	53	89			ES 1793
			50	5	6	17	26	35	57			
25.mar.15		OBDF C	28	7	8	27	44	59	100	10	12	ES 1696V
			50	5,5	6	19	28	37	61			ES 1472V
27.mar.15	Lab sample	OBDF C	28	6	7	23	37	50	85			
			50	5	5,5	16	25	34	56			
2. april 2015	Addition of 13,5 kg of Bentone to the main tank on 1st of April, accounts to 3,75 g/l	OBDF C	28	7	8	26	41	56	94	11	22	
			50	6	7	20	30	39	64	8	17	
7. april 2015		OBDF C	28	6,9	8	27	42,5	57,5	97,5	10	21,5	
			50	6	7	20	30	38,5	63	8,5	16	
8. april 2015		OBDF C	28	7	8	27	43,5	59	99	10	21,5	
			50	6,5	7,5	19,5	29	37	61	8	15-16	
9. april 2015		OBDF C	28	6	7	26	40,5	55	94	10	21,4	
			50	6	7	19,5	29	38,5	62,4	8	16	ES 1601
10. april 2015		OBDF C	28	6,5	8	27	43	59	100	10	24	
			50	6	6,5	19,5	29,5	39	63	8	17	ES 1808
13. april 2015	Added 300L of OBM B to the main tank	OBDF C	50	5	6	18	27	36	59			
15. april 2015		OBDF C	50	6	7	18	28	37	61			ES 1473
16. april 2015		ODBF C	28	7	8,5	27	43,5	60	104	9,5	32	
			50	6	6,5	20	30	40	65	8,5	22,5	ES 1999
17. april 2015		OBDF C	28	7	8	26	42	57	99	9	30	
			50	5,5	6	19	29	38	63	8	21	ES 1818
20. april 2015		OBDF C	28	6,5	7	26	42	56	96	14	24	
			50	5	6	18	28	37	61	12	18	ES1929
21. april 2015	Problems w/separation unit, fluid standing still, no experim	OBDF C										
23. april 2015		OBDF C	28	6	7	25	42	57	97	13	23	
			50	5	6	17,5	27	36	60	9	16	ES 1990
24. april 2015	250L of fluid were added to the mian tank by Ali	OBDF C	50	4,5	5	16	25	32	54			
24. april 2015	Lab sample: added 1,3g bentone to 400ml fluid		50	6	6,5	19	29	39	63,5			
24. april 2015	Sneha and Benjamin added 12 kg of Bentone to the main tank, circulation for 90 min		50	6	6,5	18	28	37	61	9	18	ES1730
24. april 2015	It was detected that not all of the bentone had mixed with the fluid. The rest was then mixed and circulated for 30		50	6	6,5	19	29	38,5	63	10	20	
27. april 2015		OBDF C	28	7	8	28	46	63	117	11	28	
			50	6	6,5	19	29	39	64	9	19	ES1934

Appendix C – MATLAB program for estimation of pressure drop

This program calculates the following parameters for laminar flow:

- Effective viscosity
- Reynolds number
- Critical Reynolds number
- Pressure drop in concentric annulus
- Pressure drop in eccentric annulus

	Start	
	clear	-Clears memory for any assigned values
		-Give appropriate values to the parameters:
	k=0.083527384;	-Consistency index, k
	n=0.87605;	-Flow index, n
	b=1.6576;	-Yield stress, b (τ_y)
	v=0.55;	-Flow velocity in the annulus, v
	Do=0.1;	-Outer diameter in the annulus, Do
	Di=0.0508;	-Inner diameter in the annulus, Di
	x=3:0.1:19;	-Interval of possible solutions for shear stress at the wall (given by x), where one expects to find the solution (in this particular case it will search from 3 to 19 and plot with a precision down to 0.1)
1	**tauw=func1(x,k,n,b,v,Do,Di)**	-Returns a plot with τ_{wall} -values and the solution of the implicit equation.
2	**visc=func2(tauw,v,Do,Di)**	-Returns the calculated value of effective viscosity, μ_{eff}
3	**re=func3(tauw,v)**	-Returns the calculated value of Reynolds number
4	**recr=func4(n)**	-Returns the value of the critical Reynolds number, at which the transitional flow starts occurring
5	**pdropc=func5(tauw,Do,Di)**	-Returns the calculated value of Pressure drop in concentric annulus
6	**pdrope=func6(tauw,Do,Di,n)**	-Returns the calculated value of Pressure drop in eccentric annulus
	End	

The code above assigns input values that are necessary for the program, eventual additional parameters are requested by the functions in the command line once the program is run. After defining the input variables only the first function is compulsory. The other functions (2-6) are free of choice, depending on the parameters the user wants to compute. The program will further call in the chosen functions (one at a time) that will calculate the corresponding parameters.

To run the program for several values of v (fluid velocity):
After running the program once for one value of v and calculating the required parameters, simply assign a new value to the input parameter v (the other input parameters remain unchanged). The functions can now be run again with the unchanged code.

Functions needed for the MATLAB program:

1. Function that solves the implicit equation for the shear rate at wall, τ_{wall}

```
function tauw = func1(x,k,n,b,v,Do,Di)
a=0.5*(Do-Di);
z=((2.*k.^(1./n).*(n+1).*v)./(a.*n.*(1-b./x).^(1+1./n).*((1-
b./x).*(n+1)./(2.*n+1)+b./x))).^n;
s=z-x;
plot(x,s)
xlabel('Interval of tau,wall values')
ylabel('Implicit equation solution is at tau,wall that gives zero')
tauw=interp1(s,x,0);
end
```

This function calculates τ_{wall} for each value of x in the given interval. It returns a graphical plot (Figure 36) for better understanding of the calculation process and finds the solution of the implicit equation (where the graph crosses the x-axis at y=0). Alternatively, fzero-function can be used to find the solution, but using this function requires a good initial guess. For all tested cases, "tauw=interp1(s,x,0)" performed best.

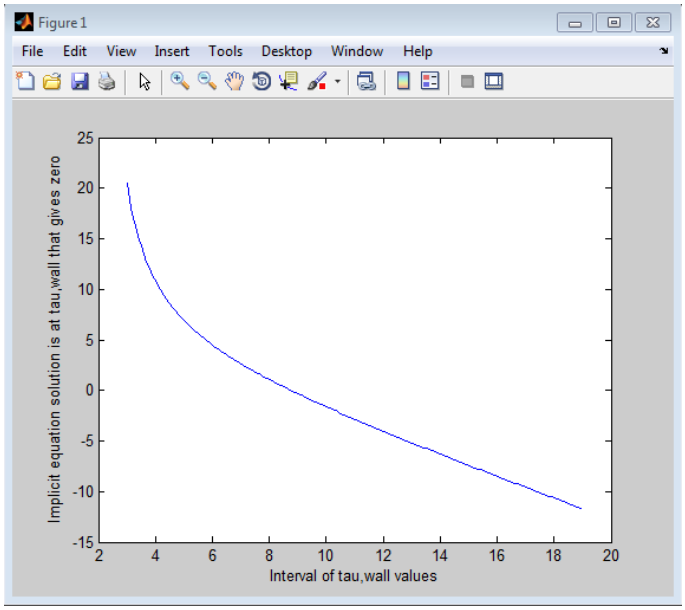

Figure 36: Solution of the implicit equation in MATLAB

2. Function that calculates the effective viscosity, μ_{eff}

```
function visc = func2(tauw,v,Do,Di)
a=0.5*(Do-Di);
visc=a*tauw/(6*v);
end
```

This function calculates the annular gap for a concentric annulus, "a" that is necessary for calculation of the effective viscosity and returns the value of μ_{eff}.

3. Function that calculates the Reynolds number for the actual flow, Re

```
function re = func3(tauw,v)
prompt = 'What is the value of the fluid density in [g/L] or [kg/m3]
(use "." for comma)? ';
rho = input(prompt);
re=12*rho*v^2/tauw;
end
```

This function calculates the Reynolds number for the actual flow. In order to confirm that the flow is laminar, this value needs to be lower than the critical Reynolds number, calculated in function 4.

4. Function that calculates the critical Reynolds number, Re_{cr}

```
function Recritical = func4(n)
Recritical=3470-1370*n;
end
```

This function calculates the critical Reynolds number, $Re_{cr,}$ at which transitional flow starts occurring.

5. Function that calculates the pressure drop in concentric annulus

```
function Pdropconcentric = func5(tauw,Do,Di)
a=0.5*(Do-Di);
Pdropconcentric=2*tauw/a;
end
```

This function calculates the annular gap for a concentric annulus, “a” that is necessary for calculation of pressure drop and returns the value of dp/dx in concentric annulus.

6. Function that calculates the pressure drop in eccentric annulus

```
function Pdropeccentric = func6(tauw,Do,Di,n)
a=0.5*(Do-Di);
prompt = 'What is the level of string eccentricity in the annulus
from 0 to 1 (use "." for comma)? ';
e = input(prompt);
Pdropconcentric=2*tauw/a;
R=1.0-0.072*(e/n)*(Di/Do)^0.8454-
3/2*(e^2*sqrt(n))*(Di/Do)^0.1852+0.96*e^3*sqrt(n)*(Di/Do)^0.2527;
Pdropeccentric=Pdropconcentric*R;
end
```

This function calculates first the annular gap for a concentric annulus, “a”. Then it calculates the pressure drop in a concentric annulus, the correction factor, R for the eccentricity and finally returns the value of dp/dx in eccentric annulus.

(Brent 1973)
(Forsythe 1976)

Appendix D – Calculated parameters for pressure drop predictions

OBM B 28C, Herschel-Bulkley model fitting							Experimental data
k=0,062122	n=0,8759	Ty=1,73073	rho=1258				
v [m/s]	tau,w [Pa]	My,eff	Re,eff	Re,crit	dp/dx ecc	dp/dx con	dp/dx ecc [Pa/m]
0,55	7,306	0,0537	633,7	2270	276,8	585,8	338,4
0,75	8,6961	0,0475	976,5		334,0	707,0	441,0
1,00	10,4836	0,043	1440		402,6	852,3	584,1
1,20	11,8702	0,0406	1831		455,9	965,1	698,5

Table 12: Estimation of pressure drop for OBM B by narrow slot approximation for HB fluids, solved in MATLAB.

OBM C 28C, Herschel-Bulkley fitting for data from April 2 and 7							Experimental data
k=0,144892	n=0,828506	Ty=2,83713	rho=1260				
v [m/s]	tau,w [Pa]	My,eff	Re,eff	Re,crit	dp/dx ecc	dp/dx con	dp/dx ecc [Pa/m]
0,3	9,3457	0,1277	145,6		367	759,8	411,4
0,5		0,1002	309,2		480	994	522,6
0,7		0,0872	497,8	2335	584,4	1210	636,5
0,9		0,0793	703,7		683,3	1415	775,8
1,1		0,0739	922,8		778,4	1612	908,6

Table 13: Estimation of pressure drop for OBM C by narrow slot approximation for HB fluids, solved in MATLAB.

Appendix E – Paper submitted to the Nordic Rheology Society

Establishing an Experimental Pre-conditioning Procedure for Rheological Characterization of Oil Based Drilling Fluids

Dias Assembayev[1], Velaug Myrseth[2], Benjamin Werner[1], Knud Richard Gyland[3], Arild Saasen[4,5], Zalpato Ibragimova[6], Jan David Ytrehus[2]

[1]Norwegian University of Science and Technology, Trondheim, Norway
[2]SINTEF Petroleum Research, Bergen and Trondheim, Norway
[3]Schlumberger Norge AS, M-I SWACO, Stavanger, Norway
[4]DetNorske, Oslo, Norway
[5]University of Stavanger, Stavanger, Norway
[6]Statoil, Bergen, Norway

ABSTRACT

In the oil industry, the ISO 10416/ISO 10414-2 standards which are used for determination of rheological properties of oil based drilling fluids do not in detail specify how the fluids should be pre-treated before measurements. In this study, a systematic approach is used to quantify the influence of waiting time and/or pre-shearing on measurements of viscosity and other rheological properties of an oil based drilling fluid.

INTRODUCTION

Oil based drilling fluids (OBDFs) are thixotropic fluids, meaning that their properties may change with time. One also knows that the fluid properties of OBDFs are highly dependent on shear history. As a result of this, it is important to have a consistent procedure for how to treat the fluids prior to measurements. This is vital to be able to compare experimentally determined flow properties, not only in this project but also to enable comparison of results between labs.

Fluids involved in oil industry drilling operations range from sea water and drilling fluids to well cements. Well cements are chemically reactive with a pump ability time that has to be adjusted to the practical pumping operation. Therefore, to be able to evaluate the viscous properties of the well cement slurries, strict preconditioning procedures exist to simulate the shear history of a cement prior to entering the annulus. These procedures include how to mix the cements slurry followed by a detailed procedure how to measure the viscosity. These procedures can be found in publications by Guillot[a] and by Dargaud and Boukhelifa[b] or in API Recommended Practices[c].

For the drilling fluid industry, a similar degree of detailed procedures does not exist for determination of the fluid viscosity values. The ISO 10414/ API 13B-2[d] and ISO 10414/API 13I[e] standards are used for determination of viscosity and gel strength of drilling fluids by use of direct-indicating viscometers (Fann 35 viscometers). However, the drilling fluid standards do not in detail specify how the fluids should be pretreated before measurements. Often the pretreatment only consists of simply shearing the sample for a specific time at 1022 s^{-1} as performed by for example

Maxey et al.[f] who sheared the sample for two minutes at their measurement temperature. Further, if one wants to compare results from Fann 35 viscometers to measurements done on a rheometer, it is even more important to have a consistent pretreatment of the fluids. The questions one seeks to answer in the present study are: i) how large is the effect of pre-shearing/no preshearing/rest?; ii) is pre-shearing or rest the most preferable in order to get reproducible results? These questions are likely to become even more important if other rheological properties than viscosity are evaluated.

Bui et al.[g] presented a study about rheological properties of oil based drilling fluids. The preparation procedures are not thoroughly described in the article. However, Bui[h] presented this preparation in some more detail. In summary his procedure was to blend the drilling fluid portion, shear it at 1000 s^{-1} for 10 minutes and then let it rest statically for a definite time period. This time period was determined by measuring the linear viscoelastic properties to determine the time to reach an accepted level of stationary values. This time was then used in the other experiments.

Understanding the effect on rheological properties of drilling fluids based on activities performed before the measurements are taken is important also in the field. In practice there are fluid data taken during different activities such as: drilling & circulation (high shear), tripping in/out (low shear), reserve volume preparations (low to no shear), etc. These data are often put in the same context and one searches for changes to the fluid based on trend analysis. Also knowing that the activity level on a drilling rig is high, the time from sampling until the measurements are done in the laboratory are varying and rarely documented. In this work, effects are identified which may increase the variance of the data and also lead to wrong interpretation of data and trends if these effects are not fully understood.

In the following, a methodical study is presented in which the effect of waiting time and/or preshearing on measurements of viscosity and other rheological properties of an oil based drilling fluid is quantified in a systematic way. These results give a foundation for a suggestion for an experimental preconditioning procedure for rheological characterization of oil based drilling fluids.

EXPERIMENTAL

Drilling fluid design

The fluid selection was based on previous work[i] and delivered by M-I SWACO. The oil based drilling fluid (OBDF) was a field fluid which had been used during actual drilling operations. Prior to delivery, the fluid was cleaned and reconditioned and then shipped to the esearch facilities of SINTEF. The OBDF is an emulsion of high alkaline brine droplets in the continuous phase of base oil, and enriched with barite weight material as well as clay (Bentone128), emulsifier and fluid loss material. Bentone128 was used as the primary viscosifier. The original ratio of base oil to water, before clay addition, was 85/15. The fluid was used for circulation in a full scale flow loop, and while running through the sand removal filters of the circulation unit both sand, clay and small amounts of water were filtered out on each circulation. This, together with evaporation effects lead to loss of water and a change in the oil/water ratio over time. This dewatering effect was noticed over a few days of operation, but it was decided to continue with the operation and keeping the viscosity expressed with Fann 35 measurements more or less constant. Bentone128 was added to compensate for the loss in viscosity, and at the respective time of sampling for the data measurements

in this work, the oil/water ratio (OWR) of the fluid was 91/9 for the first batch and 95/5 for the last batch.

Fluid characterization

Three batches of the OBDF were sampled from the flow loop at different times. The first two batches were sampled on March 20th (OWR 91/9) and April 8th 2015 and used for experiments on the Fann 35 viscometer. The third batch was sampled on April 20th 2015 (OWR 95/5) and used for measurements in the Anton Paar Physica MCR302. It should be emphasized that even though the three fluid batches might have slightly different OWR, the rheological properties of the batches are nearly identical.

Density measurements for the OBDFs were done by a standard Brand pycnometer All three batches were measured to 1,26±0,01 g/ml.

OWR was measured by retort solids analysis, ref to ISO 10414-2/API Recommended Practice 13B-2.

The effects of waiting time and/or pre-shearing were studied using the following time test matrix for measurements: immediately and after 1 hr, 2 hr, 4 hr, 6 hr, 8 hr and 24 hr resting. All measurements were performed both at 28 °C and at 50 °C, and the samples for 28 °C testing were stored at room temperature (approx. 20 °C), and the samples for 50 °C testing were stored in a heat cabinet at 38-42 °C. The whole matrix was repeated a second time with 10 min pre-shear preceding each measurement. The full test matrix was conducted both using a Fann 35 viscometer and an Anton Paar Physica MCR302 rheometer.

For the Fann 35 viscometer, measurements were started immediately after sampling from the active flow loop. The measuring cup was heated to the required temperature by use of OFITE Thermocup 130-38-25. Temperature was at all times observed by use of Eurotherm 2408i Indicator unit, with precision down to 0,01 °C. Viscosity and gel strength was measured following the ISO 10414-2/API 13B-2 and ISO 10416/2008. (600 -300-200-100-6-3 rpm, 10 sec and 10 min gel). For the preshearing measurement sequence, a shear rate of 600 rpm was applied for 10 min before starting the measuring sequence.

The MCR302 rheometer is equipped with an electrically heated temperature chamber. Before each test, temperature was set with an accuracy of 0.01 °C. After reaching set temperature, an additional 4-5 minutes waiting time were added to ensure temperature equilibrium. A concentric cylinder measuring system (CC27) was chosen to avoid evaporation at 50 °C, and the sample was changed for each new measurement. The fluid batches were mixed thoroughly every morning in a Hamilton Beach blender, at appr. 13000 rpm for 10 minutes. The measuring sequences following the previously described test matrix were then conducted immediately after mixing (for both 28 and 50 °C). For each slot in the test matrix, flow curves and amplitude sweeps were performed. Flow curves (controlled shear rate) were recorded from shear rate 1 to 1200 s^{-1}. The amplitude sweep tests were conducted with a constant frequency of 10 s^{-1} and with increasing strain from 0.001 to 100 %. The whole test sequence was then repeated with a 10 min preshear at 1000 s^{-1} before each measurement. This shear rate corresponds to 600 rpm shear in the Fann viscometer.

RESULTS

Figures 1 and 3 show dial readings in the Fann 35 viscometer for 28 and 50 °C, respectively, with no preshearing. For both temperatures, dial readings are slightly increasing with increasing waiting time, especially for rotational speeds of 600 to 100 rpm. A maximum structure build-up of 9 % for the 600 rpm reading at 28 °C and 12 % at 50 °C can be seen for the 24 hour time

period. For the readings of 300, 200 and 100 rpm the structure build-up accounts to 2 – 10 %. The 6 and 3 rpm measurements appear rather stable as well as the 10 sec and 10 min gel strength measurements. This may be explained by the fact that at the time of these last readings, the fluid has already been sheared significantly (through the 600 to 100 rpm measurements).

Fann 35 dial readings, for which the fluid has been pre-sheared for 10 min at 600 rpm (equivalent to 1022 s^{-1}) prior to measurements, are shown in Fig. 2 and 4 for 28 and 50 °C, respectively. A much flatter trend with increasing time from sampling is apparent *with* preshearing than *without* pre-shearing. Maximum structure build-up values are 4 % (600 rpm) for 28 °C and 5 % (200 rpm) for 50 °C, see Fig. 2 and 4. In Fig. 4 the measurements after 2 hours deviate clearly from the rest. There is no apparent explanation for this and these measurements are considered less reliable. Note that readings after 24 hours show a higher value than the starting value, indicating that after 24 hours waiting time pre-shearing does not reproduce the initial state. The 10 s and 10 min gel strength measurements are nearly unaffected by the preshearing. Comparison of Fig. 1 and 2, and Fig. 3 and 4, shows that preshearing gives more reproducible results than not pre-shearing, at least within a time frame of 6-8 hours after sampling.

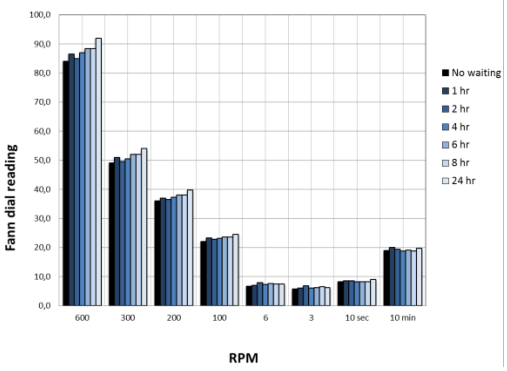

Figure 1. Fann 35 dial readings directly from resting after indicated waiting time. T= 28 °C. The lighter the colors, the longer the waiting times.

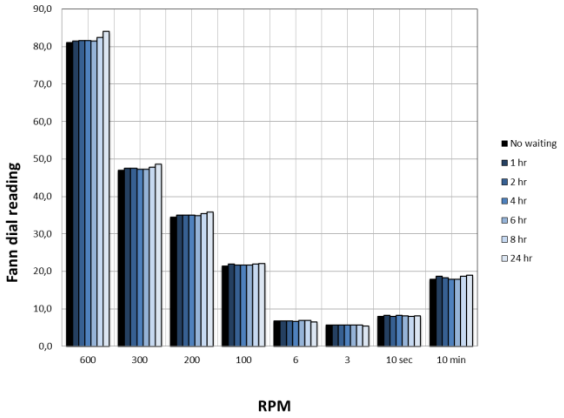

Figure 2. Fann 35 dial readings after indicated waiting time and 10 min preshearing. T= 28 °C. The lighter the colors, the longer the waiting times.

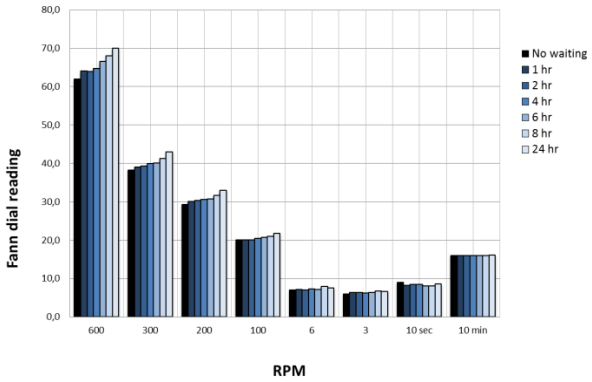

Figure 3. Fann 35 dial readings directly from resting after indicated waiting time. T= 50 °C. The lighter the colors, the longer the waiting times.

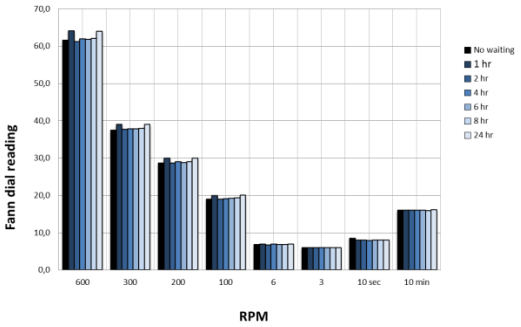

Figure 4. Fann 35 dial readings after indicated waiting time and 10 min preshearing. T= 50 °C. The lighter the colors, the longer the waiting times.

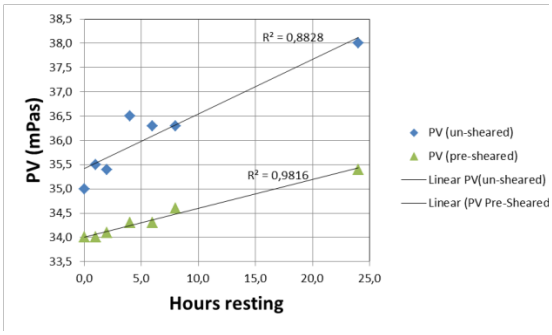

Figure 5. Plastic viscosity (mPas) plotted against resting time (h) for the non-presheared (diamonds) and the presheared (triangles) data. A linear fit is made to both data sets.

Primary aim the evaluation of the Fann 35 data is based on the high shear values (600 and 300 rpm). These two data points are in the field expressed by the Plastic Viscosity (PV) through the Bingham Plastic model, assuming a near constant viscosity at high shear rates. The PV of a drilling fluid is described physically as the forces/friction between the interactions of non-continuous particles in the invert fluid, solids & brine droplets, creating a weak structure. Plotting the PV of the fluids towards the waiting time (see Fig. 5) shows for the 50 °C measurements an increasing trend (3 whole digits) the first 8 hours and then a flattening trend up to 24 hours. For the 28 °C measurements, this flattening trend after some hours is not that evident. Preshearing removes this effect seen at 50°C, but as can be seen in both graphs of the pre-sheared fluids there is a linear increase in PV over 1 digit approximately (the 1 hour value at 50 °C pre-shared disclaimed as an outlier). As the PV is believed to describe the friction at high shear of the particles, content, size and shape will have an impact, and size in particular. It is not believed that the weighting material or other solids in this short period of time is aggregating to form larger sized particles. But the internal phase consists of droplets that are highly attractive to each other, and kept dispersed in the continuous phase by the emulsifier in the system. If the emulsion is weakened over this period due to the lack of shear, the size of the internal phase droplets will increase due to aggregation of the water phase. This can lead to a higher friction between the droplets and hence a higher PV.

Figures 6 and 7 show flow curves measured in the Anton Paar rheometer, at 28 and 50 °C, respectively. The top bunch of lines in the figures represent flow curves with no preshearing. In Fig. 5, the structure build-up with no preshear at 28 °C is clearly visible with increasing waiting times. The lower bunch of lines, representing measurements with pre-shear fall almost on top of each other, i.e. the same trend is apparent here as for the Fann measurements. The measurement for 8 hour rest and preshear clearly deviates from the rest and is considered an outlier.

Figure 7 shows the same measurements done at 50 °C. At this temperature the structure regeneration with no preshear is much less pronounced, and the difference between the presheared and not presheared measurements is small. In other words, at 50 °C preshearing has no significant influence on the flow curves.

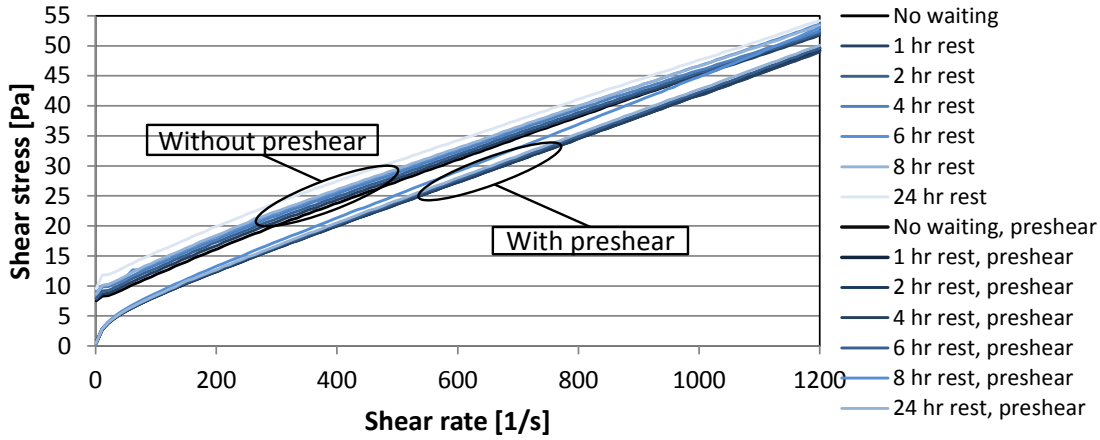

Figure 6. Flow curves of the OBDF for the non-presheared and the presheared samples at 28 ºC. The lighter colors represent longer waiting times.

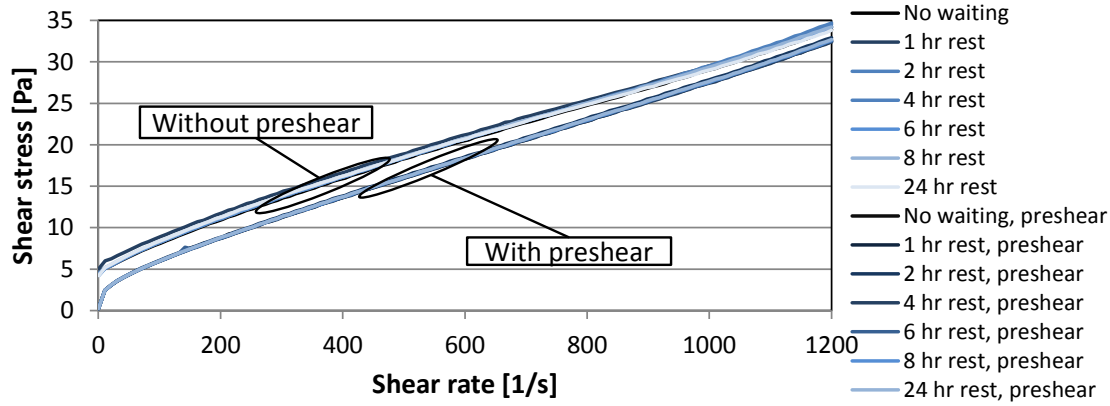

Figure 7. Flow curves of the OBDF for the non-presheared and the presheared samples at 50 ºC. The lighter colors represent longer waiting times.

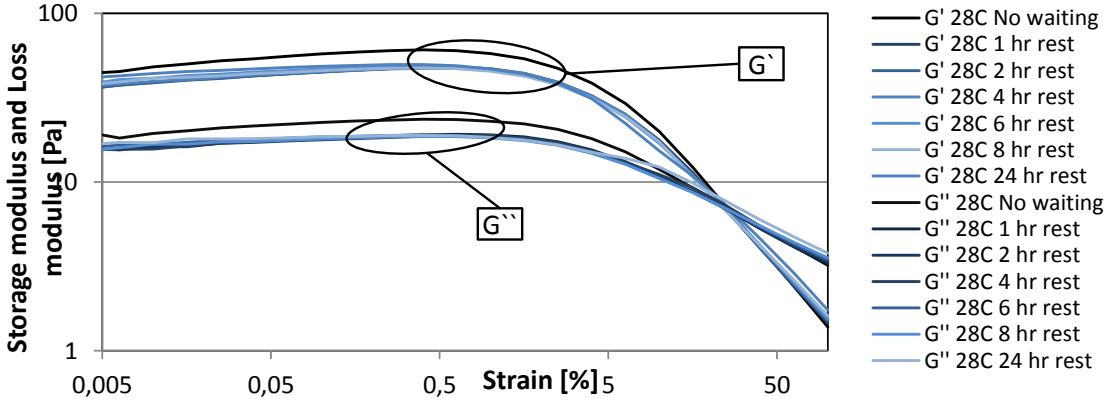

Figure 8. Amplitude sweeps of the OBDF for the non-presheared sample, at 28 ºC. Storage modulus (G') and loss modulus (G") are marked in the figure. The lighter colors represent longer waiting times.

Figure 8 shows the storage (G') and loss modulus (G'') of a strain sweep performed at a frequency of 10 Hz at 28 °C, with no preshear. The measurement made immediately after mixing deviates from the others. Comparison with Fig. 9, showing the same measurement with 10 min preshearing at 1000 s^{-1}, reveals that preshearing gives more reproducible results, even after 24 hours waiting time. Pre-shearing has no effect on the G'/G'' cross-over point (flow point) but the end of the linear viscoelastic range (LVER) is moved to higher strain values, i.e. the fluid tolerates a higher strain with preshear before the structure starts to break down than it does with no preshear. For 50 °C (Figs. 10 and 11), the picture is slightly different. Preshearing produces results much more similar than does no pre-shearing, but G'/G'' cross-over point is moved significantly to higher strain values. End of LVER is also moved to higher strain values with preshear than with no preshear. In other words, amplitude sweeps at 50 °C are more sensitive to preshear than at 28 °C.

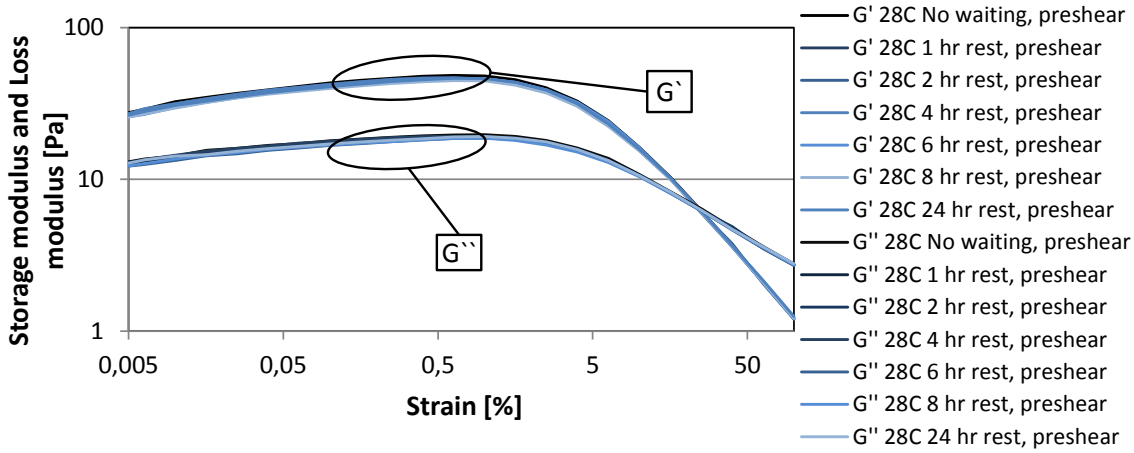

Figure 9. Amplitude sweeps of the OBDF for the presheared sample, at 28 °C. Storage modulus (G') and loss modulus (G'') are marked in the figure. The lighter colors represent longer waiting times.

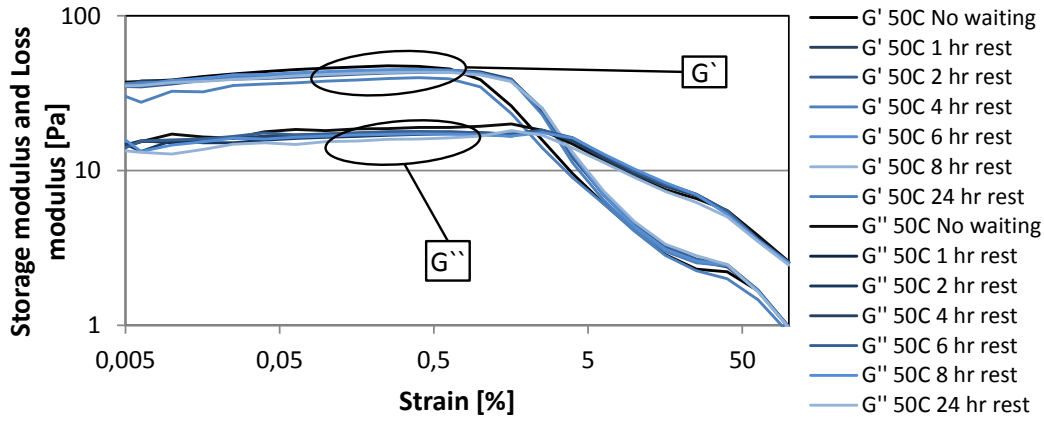

Figure 10. Amplitude sweeps of the OBDF for the non-presheared sample, at 50 °C. Storage modulus (G') and loss modulus (G'') are marked in the figure. The lighter colors represent longer waiting times.

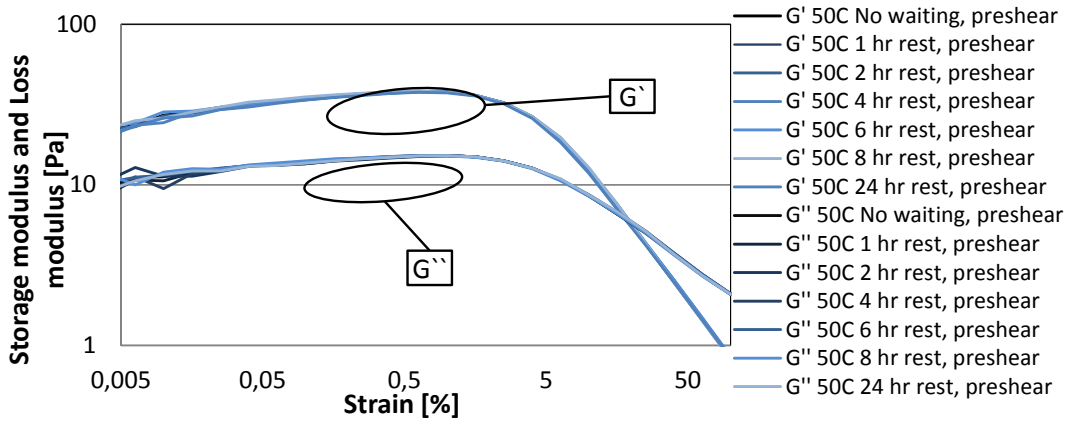

Figure 11. Amplitude sweeps of the OBDF for the presheared sample, at 50 °C. Storage modulus (G') and loss modulus (G") are marked in the figure. The lighter colors represent longer waiting times.

DISCUSSION

. In this study, the samples have been exposed to 10 min preshearing at 1000 s^{-1}. The effect of preshearing for a shorter or longer time or at a different shear stress has not been tested. It is possible that shearing for a longer time would give even more reproducible results. At the same time, waiting before testing is a non-productive time, which would increase inefficiency and costs, especially in the field. Also, given that 10 min preshear is given in ISO/API standards, we suppose that 10 min preshear is a good compromise.

Many results from this study are according to expectations, although to our knowledge there are no publications where the effects have been systematically quantified before. The results from this study is proposed as practical guidelines to measurements of viscosity and other rheological properties. The effect of waiting time and/or pre-shear should be tested for each individual fluid, but it is expected that these results will be valid for most oil based drilling fluids.

CONCLUSIONS

In summary, the main conclusions are:

- For both temperatures, one gets more reproducible results with preshearing, except for the 24 h measurements. Even with preshearing, sample readings change after 8 hours and/or 24 hours.
- Most findings are as expected, but the effects are now quantified for both simple viscosity measurements (direct-reading viscometer) and for measurements of visco-elastic properties (rheometer). The findings may serve as a methodic reference work and a practical guide.
- Viscoelastic properties are even more sensitive to preshearing at 50 ^{0}C than at 28 ^{0} C. Viscous properties are less temperature sensitive with regards to preshearing.
- For comparative data, preshearing is recommended to get more reproducible results.
- For in-depth characterization of rheological properties, preshearing is not recommended as viscoelastic properties are significantly affected by preshear, especially for higher temperatures.

ACKNOWLEDGMENTS

This work is carried out at the SINTEF fluid laboratories in Bergen and Trondheim. Financial support from the Norwegian research council (NRC), Det Norske and Statoil is greatfully acknowledged. The project "Hole Cleaning Performance" is financed through the PetromaxII research program in NRC. The authors thank M-I Swaco for providing chemicals and technical advice.

REFERENCES

a. Guillot, D., "Rheology and Flow of Well Cement Slurries". In Nelson, E. and Guillot D. (eds) *Well Cementing*, Schlumberger, Sugar Land, Texas, 2006. Chapter 4.

b. Dargaud, B. and Boukhelifa, L., "Laboratory Testing, Evaluation, and Analysis of Well Cements". In Nelson, E. and Guillot D. (eds) *Well Cementing*, Schlumberger, Sugar Land, Texas, 2006. Appendix B.

c. American Petroleum Inst., *Recommended Practice for Testing Well Cements*, *API RP 10B*, 22nd ed., Washington D.C., 1999.

d. ISO 10414-reference

e. ISO 10416/API -reference

f. Maxey, J., McKinley, G., Ewoldt, R. and Winter, P. (2008), "Yield Stress: What is the "True" Value?", Paper *AADE-08-DF-HO-27*.

g. Bui, B., Saasen, A., Maxey, J., Ozbayoglu, M.E., Miska, S.Z., Yu, M. and Takach, N.E. (2012), "Viscoelastic Properties of Oil-Based Drilling Fluids", *Ann. Trans Nordic Rheol. Soc*., **20**, 33-47.

h. Bui, B. (2012), "Determination of Viscoelastic Properties of Drilling Fluids". M.Sc. thesis, University of Tulsa.

i. Oltedal, V.M., Werner, B., Lund, B., Saasen, A., and Ytrehus, J.D. (2015), "Rheological properties of oil based drilling fluids and base oils", Paper *OMAE2015-41911*.

Appendix F – Contribution to other works

Proceedings of the ASME 2015 34th International Conference on Ocean, Offshore and Arctic Engineering
OMAE2015
May 31- June 5, 2015, St. John's, Newfoundland, Canada

OMAE2015-41911

RHEOLOGICAL PROPERTIES OF OIL BASED DRILLING FLUIDS AND BASE OILS

Velaug Myrseth Oltedal
SINTEF Petroleum Research
Bergen, Norway
Email: Velaug.Oltedal@sintef.no

Benjamin Werner
Norwegian University of Science and Technology
Trondheim, Norway
Email: Benjamin.Werner@ntnu.no

Bjørnar Lund
SINTEF Petroleum Research
Trondheim, Norway
Email: Bjornar.Lund@sintef.no

Arild Saasen
Det Norske, Oslo, Norway/
University of Stavanger,
Stavanger, Norway
Email: Arild.Saasen@detnor.no

Jan David Ytrehus
SINTEF Petroleum Research
Trondheim, Norway
Email:
JanDavid.Ytrehus@sintef.no

ABSTRACT

Drilling fluids for oil wells must meet a number of requirements, including maintaining formation integrity, lubricating the drill string, and transporting cuttings to the surface. In order to satisfy these needs, drilling fluids have become increasingly complex and expensive. To ensure safe and efficient drilling, it is vital for the drilling operator to be able to make a qualified choice of fluid appropriate for each individual well.

API/ISO standards specify a set of tests for characterization of drilling fluids. However, fluids that are tested to have equal properties according to these standards are still observed to perform significantly different when used in the field. The aim of the full project is to provide a thorough comparison of drilling fluids in particular with respect to hole cleaning performance, in light of the issues presented above. As part of this investigation we here present results for two oil based drilling fluids, as well as for the corresponding base oil. The drilling fluids differ in composition by varying fraction of base oil, and thus density and water content.

The fluids have been tested according to the API standard, and further, viscoelastic properties have been examined using an Anton Paar rheometer. The rheological test campaign includes determination of the linear viscoelastic range (LVER), viscosity and yield point, thixotropic time test, and temperature dependence of rheological parameters.

Further, it is demonstrated how the rheological data may be used to interpret data from ongoing full scale flow loop experiments with the same fluids. In a more general context, the rheological test campaign of the drilling fluids is expected to make a crucial contribution for the petroleum industry in explaining observed differences in hole cleaning properties beyond what todays API/ISO industry standard provides.

INTRODUCTION

Drilling fluids are complex liquids which shall serve several different purposes, such as transport of drilled materials (cuttings), cooling and lubrication of the drill bit, adequate pressure, formation integrity, avoid formation damage, and transfer hydraulic energy from surface to a downhole motor.[1,2] Drilling fluids therefore show both non-Newtonian, elastic and thixotropic behavior. In this paper we focus on the properties which are most important for cuttings transport. The pressure drop during circulation should not be too high, while still allowing adequate cuttings transport both in horizontal and inclined well sections. However, during circulation breaks, such as the insertion or removal of drill pipe sections, settling of particles should be minimized. In order to provide sufficient downhole pressure to balance the formation pressure, many drilling fluids contain small solid particles (barite particles) as weight materials. During long circulation breaks, barite sag may occur, where these particles settle towards the bottom of the vertical section and the density of the drilling fluid becomes non-uniform. The rheological properties of drilling fluids at low and vanishing shear rates are therefore important in practical applications, and most drilling fluids are therefore designed to have a nonzero yield stress τ_y, while being shear

thinning at larger shear rates. The resulting viscous properties are commonly represented by the Herschel-Bulkley model for shear stress versus shear rate

$$\tau = \tau_y + K\dot{\gamma}^n \quad (1)$$

Yield stress fluids often also show time-dependent properties; exhibiting a reversible decrease of viscosity versus time during flowing conditions. Yield stress and thixotropy are usually considered as separate phenomena, but often appear in the same fluids, and are believed to be caused by the same fundamental physics[3].

EXPERIMENTAL

Drilling fluid design

The fluid selection was based on previous work[4,5] and aimed to test fluids with comparable density and viscosity. For the experiments three fluids were delivered by MI Swaco, two batches of an oil based drilling fluid (OBDF) with densities of 1,28 and 1,5 g/ml respectively, and the corresponding base oil (BO). The OBDF had been used during actual drilling operations. Prior to delivery, the fluid was cleaned and reconditioned and then shipped to the research facilities of SINTEF in Trondheim. The OBDF is an emulsion of water droplets in base oil enriched with weight material as well as salts, clay, $Ca(OH)_2$ emulsifier, and fluid loss material. The original ratio of base oil to water, before additives, was 80/20. To be able to operate the fluids in the full scale flow loop, adjustments of the density and viscosity was necessary. The two batches of fluid, as well as base oil, were mixed to two new batches with a final density of 1,1 (OBDF A) and 1,26 (OBDF B) g/ml respectively. OBDF A has a higher oil/water ratio than OBDF B, but the exact ratio is unknown.

The base oil is a refined mineral oil. The base oil was selected due to its transparency and the aim to observe the cuttings transport in the flow loop visually via a transparent pipe section. The density of the base oil was 0,814 g/cm^3.

Fluid characterization

The fluid batches were mixed thoroughly every morning in a Waring blender, at appr. 6000 rpm for 10 minutes. The fluids were then left to rest for 1 hour, before the start of the measurements.

Density measurements for the OBDFs were done on an Anton Paar DMA 4500M densitometer and on a Coriolis flow meter. Viscoelastic properties were analyzed with Anton Paar rheometers MCR102 and MCR302. Flow curves were recorded from an initial shear rate of 1 s^{-1} to a final shear rate of 1200 s^{-1}, at 10, 28 and 50 °C. To determine the yield point, flow curves with controlled shear stress in a range of 0,1 – 100 Pa were performed. Amplitude sweep tests were conducted to estimate the linear viscoelastic range (LVER) and the storage and loss moduli. For these tests a strain range of 0,001% to 100% was selected due to the fact that an initial strain of 0,01% was probably inside the LVER. The proposed strain value from the software Rheoplus was then used to run thixotropic 3-interval time tests ORO (oscillation-rotation-oscillation) to study the time dependent structure recovery after deformation. During the first interval, the rest interval, the fluid was oscillated with the proposed strain value within the LVER, to give a reference value for the strength of the structure of the fluid. In the second interval, the load interval, the fluid was sheared with a shear rate of 1000 s^{-1} for one second. The recovery interval (third interval) was set to observe the time needed until no structure regeneration was recorded anymore, with an oscillation equal to the first interval. The frequency for both the amplitude sweeps and the thixotropy tests was 10 Hz.

For the base oil, flow curve measurements as well as a temperature sweep from 5- 50 °C were performed. The other tests were irrelevant because it is a Newtonian fluid.

All measurements were performed at 28 and 50 °C and the samples of the OBDF fluid were changed for every measurement. The concentric cylinder (CC27) measuring system was chosen to avoid evaporation of sample at higher temperatures and during the long time thixotropy measurements. All tests have been repeated 2-3 times to ensure reproducibility of the results.

All fluids have been tested with a Fann35 viscometer, according to the API/ISO standard at 28 °C, and the viscosity results are compared to the rheological data. The Fann measurements show good reproducibility.

RESULTS

Flow curves

Flow curves measured in the Anton Paar rheometer for the BO and OBDFs are shown in Fig. 1, for temperatures of 28 and 50 °C. The BO was measured at 25 and 50 °C. The BO shows the behavior of a Newtonian fluid, i.e. the viscosity is constant and not stress dependent. This can be seen in Fig. 1 as linear flow curves for the BO. At a certain shear rate, however, the flow in the viscometer annulus becomes unstable and the so-called Taylor vortices appear[6]. These smoke-ring like vortices will extract energy out of the shear flow and the reading will look like there is a more viscous fluid in the annulus. Therefore, the rheometer reading values in this unstable region have been removed for the BO curves. This is also the explanation for the apparently increasing viscosity for the OBDFs at high shear rates, from approximately 1000 s^{-1} and higher.

The drilling fluids are viscoelastic fluids, exhibiting a shear thinning behavior. This can be seen in Fig. 1 as a decreasing

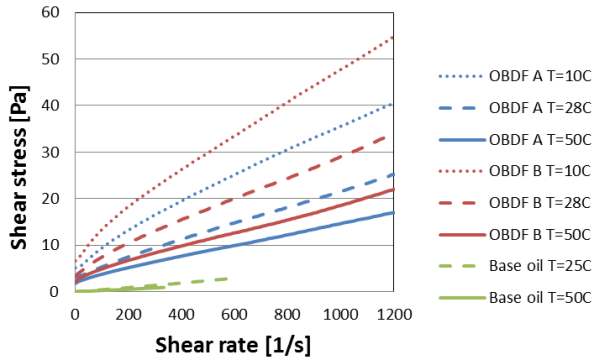

Figure 1. FLOW CURVES FOR THE OBDFs AND BO FROM SHEAR RATE 1-1200 s^{-1}.

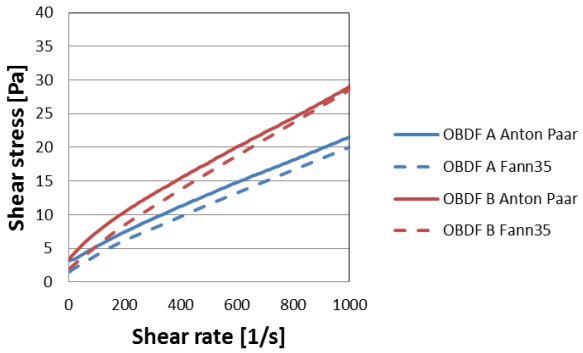

Figure 2. COMPARISON OF FANN VISCOMETER AND ANTON PAAR RHEOMETER DATA FOR OBDF A AND B AT 28 °C.

slope with increasing shear rate. The temperature dependence of the viscosity is clearly higher for the OBDFs than for the BO.

As already mentioned, at high shear rates the OBDFs appear to be shear thickening, but this is only an artefact of an unstable annulus flow. Since the BO is a Newtonian fluid, the only further measurements for the BO will be a viscosity temperature sweep.

Table 1 shows shear stress measured in the Fann viscometer for both OBDFs. Figure 2 shows a comparison of flow curves measured by the Fann viscometer and the Anton Paar rheometer for OBDF A and B at 28 °C. The deviation between the two sets of measurements is small but significant. For OBDF A, the deviation is approximately constant over all shear rates, while for OBDF B the deviation is higher for smaller shear rates. For high shear rates, the Fann and Anton Paar values are almost equal for OBDF B.

Table 1. SHEAR STRESS (Pa) FOR THE OBDFs MEASURED IN THE FANN VISCOMETER AT T=28 ^{0}C. CONVERSION FACTOR USED WAS: 1 lbf/100 ft^2 = 0,51 Pa.

Fann speed (rpm)	*3*	*6*	*100*	*200*	*300*	*600*
OBDF A (Pa)	1,5	1,8	5,6	8,7	11,7	20,4
OBDF B (Pa)	2,0	2,3	7,7	12,2	16,6	29,1

Temperature sweeps

Figure 3 shows viscosity temperature sweeps for the OBDFs and the base oil. As expected, both fluids show a large temperature influence of the viscosity. The viscosity of the higher density fluid, OBDF B, is more influenced by an increase in temperature than is OBDF A.

The temperature dependence of the fluids was compared with an Arrhenius-type model (see Fig. 4)

$$\mu = \mu_0 \exp\left(\frac{E}{RT}\right) \tag{2}$$

and with an exponential type model. It is found that the temperature dependence of the viscosity for the OBDFs is more complex than indicated by either of these models, whereas the base oil fits well to the Arrhenius model as seen in Fig. 4.

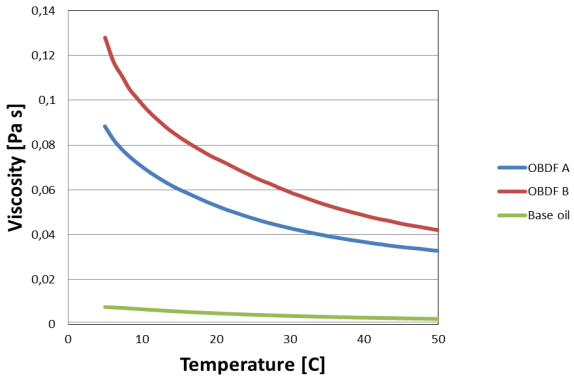

Figure 3. TEMPERATURE SWEEPS OF THE OBDFs AND THE BO AT A TEMPERATURE RAMP OF 1 °C/MIN AND SHEAR RATE OF 100 s^{-1}.

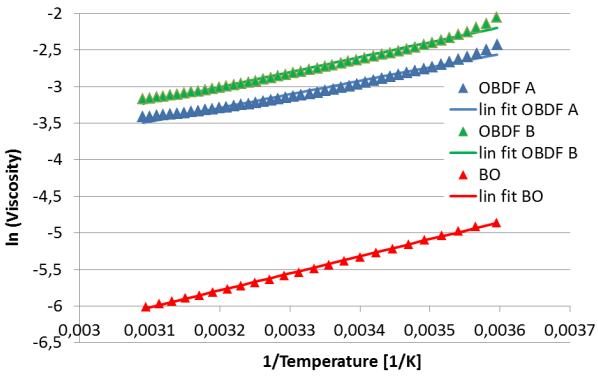

Figure 4. COMPARING TEMPERATURE DEPENDENCE OF THE OBDFs AND BASE OIL WITH THE ARRHENIUS MODEL.

Determination of yield point

Determination of the yield point was performed for the OBDFs by three different methods using the Anton Paar rheometer. In the first method (M1), a shear stress sweep is performed, where the stress is ramped in a logarithmic manner from low stress until a flow regime is well developed. A plot of strain vs shear stress is plotted in Fig. 5 for the two fluids and two temperatures. The yield point of the fluid is where the strain-stress curve deflects from linearity, and is marked in the figure and tabulated in Tab. 2. At 28 °C, there is not much difference between OBDF A and B, and the yield point values are quite low, around 2 Pa. For the 50 °C measurement, the yield point values are lower, as expected for higher temperatures. OBDF A has slightly lower yield point at 50 °C than does OBDF B.

Table 2: YIELD POINTS OF THE OBDFs DETERMINED BY THREE DIFFERENT METHODS, M1, M2, AND M3, AS WELL AS FROM FANN MEASUREMENTS. T=28 AND 50 °C.

Fluid	OBDF A		OBDF B	
Temperature (°C)	*28*	*50*	*28*	*50*
Yield point M1 (Pa)	2,1	1,4	2,0	1,7
Yield point M2 (Pa)	2,9	1,8	3,3	2,2
Yield point M3 (Pa)	0,61	0,05	0,95	0,12
Yield point Fann (Pa)	1,6	-	1,7	-

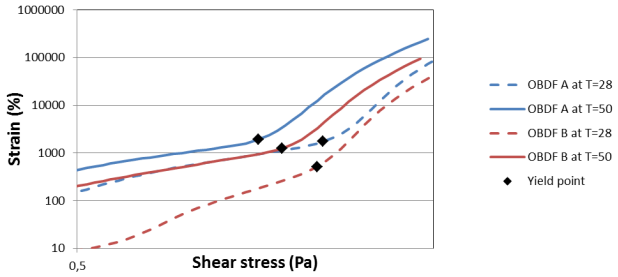

Figure 5. SHEAR STRESS SWEEPS FROM 0,1-100 Pa FOR OBDF A AND B AT T=28 AND 50 °C. ONLY THE AREA WHERE THE CURVES DEFLECT FROM LINEARITY IS SHOWN IN THE FIGURE.

The second method (M2) involves matching the flow curves with a regression model, to estimate the crossing point with the y-axis. The regression analysis was performed on the shear rate range 1-1000 s^{-1}, to match the shear rate range covered by the Fann viscometer. Both the Bingham (B_m) and the Herschel-Bulkley (H-B_m) model were used. The H-B_m is the most widely used within the petroleum industry as it is found to best describe the whole range of shear rates experienced by the drilling fluid in the well. This was also found for the fluids in the present study. In Fig. 6, the result of the modelling for OBDF A at 28 °C is shown. The H-B_m is able to represent the data well also at low shear rates. Yield points estimated from the H-B_m is presented in Tab. 2. For M2 the same trends in yield point values are seen as for M1. OBDF A has lower yield point than OBDF B, and with increasing temperature the yield point values decrease for both fluids.

Yield points estimated from the B_m model (not shown) are slightly higher but generally in good agreement with H-B_m.

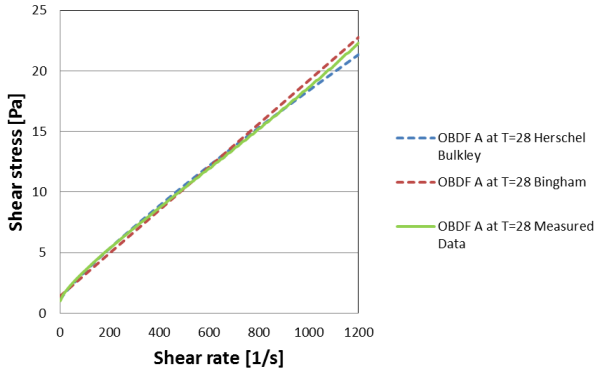

Figure 6. FLOW CURVE FOR THE OBDF A AT 28 °C FITTED BY THE BINGHAM AND THE HERSCHEL-BULKLEY MODEL.

The Herschel-Bulkley parameters, including the yield point, were also determined by a least squares fitting using the Fann viscometer data for OBDF A and OBDF B. The matched yield stress values were 1.6 Pa and 1.7 Pa, respectively, and these values agree well with the other yield points listed in Tab. 2.

The third method (M3) is described in the next section.

Amplitude sweeps

Figures 7 and 8 show amplitude sweeps for the OBDFs at 28 and 50 °C. The strength of the storage modulus, G', relative to the loss modulus, G", gives information about the stiffness of a material. The length of the linear viscoelastic range (LVER) indicates how large strain the fluid tolerates before the internal structure of the fluid starts to break.

For both temperatures, the higher density fluid, OBDF B, shows the longer LVER, indicating that increased density and/or increased water content leads to a higher tolerance for strain impact. For OBDF A and B, the end of LVER values are listed in Tab. 3.

For the lighter density fluid, OBDF A, the G'/G" ratio is lower than for OBDF B, showing a weaker inner structure for lower densities/water content. The crossing point of G' and G" is often referred to as the "flow point" and is the strain value at which the fluid's inner structure is broken and the fluid starts flowing. This can also be referred to as the yield point in the context described in the previous section, and this represents our third method (M3) of determining yield points. The corresponding yield point values are tabulated in Tab. 2. For both temperatures, OBDF A has a lower flow point/yield point than OBDF B and shows a faster decomposition of the inner structure.

For both temperatures, the loss modulus develops a small peak right before the flow point, indicating that an extra network structure was present at rest. This structure might start developing microcracks before breaking down, giving rise to such an extra peak. This phenomenon is known[7] and has been seen before for water based drilling fluids[4].

Table 3. END OF LVER (%) FOR OBDF A AND B, AT TEMPERATURES 28 AND 50 °C.

End LVER	*28 °C*	*50 °C*
OBDF A	0,25%	0,06%
OBDF B	0,63 %	0,10%

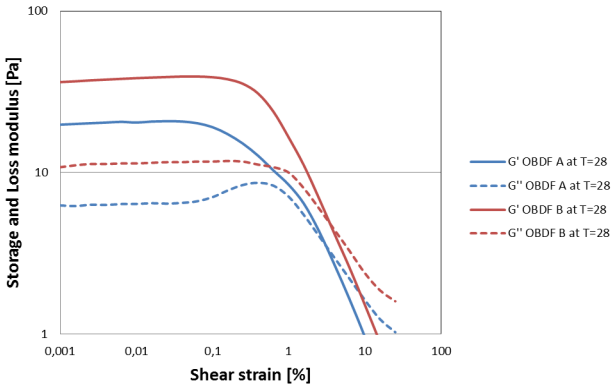

Figure 7. AMPLITUDE SWEEPS SHOWING THE STORAGE MODULI (G') AND LOSS MODULI (G") OF THE OBDFs AT A TEMPERATURE OF 28 °C, PERFORMED AT INCREASING STRAIN AND AT A FREQUENCY OF 10 s^{-1}.

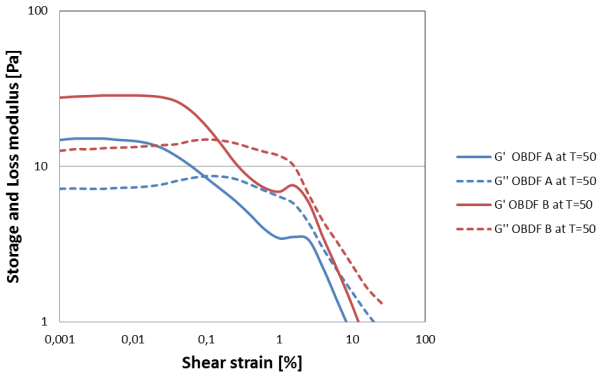

Figure 8. AMPLITUDE SWEEPS SHOWING THE STORAGE MODULI (G') AND LOSS MODULI (G") OF THE OBDFs AT A TEMPERATURE OF 50 °C, PERFORMED AT INCREASING STRAIN AND AT A FREQUENCY OF 10 s^{-1}.

Thixotropy tests

The thixotropy curves in Fig. 9 show the structure recovery of OBDF A at 28 and 50 °C. After 432 and 362 seconds, for 28 and 50 °C respectively, the elastic modulus G' has recovered to 100% of the starting value. At both temperatures the storage modulus G' exceeds the reference value from the rest interval during the recovery interval. This gain accounts to 148 % (after 2090 s) and 160 % (after 2730 s) for the 28 and 50 ^{0}C measurements, respectively.

After G' reaches a maximum, the value starts decreasing. This feature is most pronounced for the 50 ^{0}C measurement. This shows that the structure of the fluid at these temperatures is not stable within the timeframe of this test.

Thixotropy tests were performed also for OBDF B (not shown), and the same trends were found as for OBDF A.

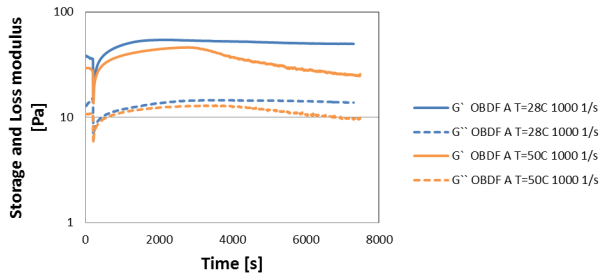

Figure 9. 3-INTERVAL THIXOTROPY TESTS (ORO) FOR OBDF A AT 28 AND 50 °C. FREQUENCY WAS 10 s^{-1}.

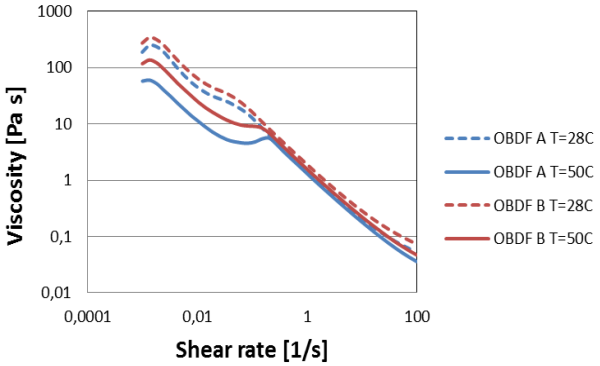

Figure 10. VISCOSITY VS SHEAR RATE FOR THE OBDF AT 28 AND 50 °C.

DISCUSSION

It is important to note that yield point is a regression parameter and not a material constant, since it depends on both the measuring method as well as on the choice of analysis or modelling method. Still, one may hold some physical significance to the yield point value, and comparison of different methods is possible. Comparing yield points determined by methods M1 and M3 reveals a good correlation. Both methods show a lowering of the yield point with increasing temperature, as expected. For the heavier fluid OBDF B the yield points are higher than for OBDF A, for both temperatures, which is consistent with a higher viscosity for OBDF B. Yield points from M2 are consistently higher than from M1 and M3, although the same trends are apparent here. M2 may be regarded as the least reliable or most coarse of the three methods investigated here.

There have been previous discussions as to whether or not oil based drilling fluids have a real yield point[8-10]. Previous studies on water based drilling fluids have revealed a well defined gel structure[4]. Water based drilling fluids consist of a blend of solids and polymers which easily form a semi-solid network. The strength of this network is what is intuitively accepted as the gel strength. For flow to start, it is necessary to break this semi-solid structure, and the motion becomes liquid like. Oil based drilling fluids are formed differently. In their simplest form these fluids are constructed as a water-in-oil emulsion. Typically, the water-oil ratio lays between 30/70 and 15/85. To further investigate this matter and the fluid structure of the OBDFs, low shear rate behaviour was mapped. Figure 10 shows a plot of viscosities of the currently investigated OBDFs measured at low shear rates going from 0,001 to 100 s^{-1}.

At very low shear rates around 0,001 s^{-s}, there is an apparent tendency towards a shear thickening behaviour. The measurement was repeated starting at shear rate 0,01 s^{-1}, and the same peak appeared also here at the beginning of the measurement, i.e. at around 0,01 s^{-1}. This indicates that this peak is more an artefact of the measurement procedure, rather than an actual shear thickening behaviour. A possible explanation for this peak is that for very low shear rates and standstill, Brownian forces tend to arrange the water droplets of the emulsion in a configuration with the longest possible distance to nearest neighbour. This results in a crystal like structure and a low viscosity. However, when these water droplets become very small, the inter-droplet distance becomes very small too. Hence, a relatively large strain can be formed before the droplets exchange their position in the structure. This can lead to a measurable linear strain amplitude region, as seen in Fig. 7 and 8. However, there are no forces except gravity that prevent the droplet to leap-frog and break that pseudo-gel structure. In addition to the water the oil based drilling fluid contains treated bentonites. The bentonite particles are surface coated to make them oil-wet. These particles are plate-like. Any strain will make these rotate. Rotation of plate-like particles require energy. Thus, the effect is observed as a significant increase in viscosity. Still, no physical semi-solid network is formed. In sum, in the sense of pressure losses the water based and oil based fluids have a similar behaviour. But in the sense of carrying particles like weight material, there are no network structures present in the oil based drilling fluids. Further measurements going in the opposite direction, from higher to lower shear rates, may further enlighten the results from Fig. 10.

We notice in Fig. 10 that there are two distinct viscosity regimes for both samples and at both temperatures, with a transition zone between 0.05 s^{-1} and 0.2 s^{-1}. A similar behaviour was observed by Herzhaft et al.[11] in a rheological study of an OBDF with different compositions (see e.g. Fig. 1 in their paper). They found a transition from a non-Newtonian behaviour at high shear rate to a Newtonian behaviour at lower shear rates, with a cross-over point which they defined as a value of unity of the Peclet number

$$Pe = \frac{6\pi\mu_o \dot{\gamma} r^3}{k_b T} \quad (3)$$

representing the ratio between Brownian or colloidal forces and hydrodynamic forces. Here, μ_o is the viscosity of the continuous phase and r is the droplet diameter, here considered as monodisperse hard spheres. This model would explain why the shear rate at the cross-over point increases with temperature.

The results from this study can be used to interpret the hydraulics and hole cleaning behavior of drilling fluids[12]. For example, although the yield stress property is most important for behavior during non-flowing conditions, it will also manifest itself in a non-zero pressure gradient required to initiate flow in a wellbore or pipe. Furthermore, the yield stress will result in two high-viscosity regions in a fully eccentric annulus (typical for a horizontal drilling situation); one plug-flow region in the wide gap, and one no-flow region in the narrow (vanishing) gap. At fairly low flow rates the flow in the lower (narrower) part of the annulus is laminar, and close to the contact point at the bottom there is a no-flow region. Consequently, when particles are transported with the fluid, particles will settle into the unsheared no-flow fluid region and cannot be entrained since there is no flow. The bed builds up until the no-flow region vanishes. If the string rotates or if there is a tangential flow due to a rifled wellbore, a no-flow region at the bottom of the pipe can be prevented and the cuttings bed buildup will be smaller. The results from the linear sweeps (measurements at controlled shear stress or controlled shear rate) are probably more representative for the study of steady state flow in a pipe, both with respect to general hydraulics and hole cleaning, than the oscillatory sweeps are. However, the latter may be important with respect to the transition to turbulence and the turbulent part of the effective viscosity and consequently relevant for hydraulics and cuttings transport. This interaction is currently poorly understood and further research, both experimental, numerical and theoretical, is needed.

CONCLUSIONS

Rheological properties of two oil based drilling fluids has been thoroughly mapped, both for the high and low shear rate regimes, as well as for the oscillation mode. Yield points were determined by several different methods, and the resulting yield point values were found to agree quite well. The origin of yield stress values for oil based versus water based drilling fluids was discussed. The viscosity of the drilling fluids is largely influenced by temperature while the base oil is only slightly influenced. Time dependence tests showed that, after high shearing, the elastic component first regenerates to a level higher than the starting point, before decreasing. Comparison of the two rheology measurement systems Fann and Anton Paar showed small but significant differences.

ACKNOWLEDGMENTS

This work is carried out at the SINTEF fluid laboratories in Bergen and Trondheim. Financial support from the Norwegian research council, Det Norske and Statoil is greatfully acknowledged. The authors thank the industry partners for contributions to technical discussions, MI Swaco for providing chemicals and technical advice, and Dias Assembayev for performing some of the measurements reported here.

REFERENCES

1. A. Saasen (1998). "Hole cleaning during deviated drilling- The effects of pump rate and rheology", paper *SPE 50582*.

2. A. Schulz, H. Strauβ, M. Reich (2013). "Modern rheological analysis of drilling fluids", paper *OMAE2013-11580*, pp. V006T11A030.

3. J. Maxey, R. Ewoldt, P. Winter, and G. McKinley (2008). "Yield Stress: What is the "True" Value?", paper *AADE-08-DF-HO-27*, AADE Fluids Conference and Exhibition 2008, Houston, USA.

4. A. Torsvik, V. Myrseth, N. Opedal, B. Lund, A. Saasen, J. D. Ytrehus (2014). "Rheological comparison of bentonite based and KCl/polymer based drilling fluids", *Ann. Trans. Nord. Rheol. Soc*., vol **22**, pp 219-224.

5. J. D. Ytrehus, A. Taghipour, B. Lund, N. Opedal, B. Werner, A. Saasen, Z. Ibragimova (2014). "Experimental study of cuttings transport efficiency of water based drilling fluids", paper *OMAE2014-23960*.

6. G. I. Taylor (1923). "Stability of a Viscous Liquid Contained Between Two Rotating Cylinders," *Philos. Trans. R. Soc. London, Ser. A*, vol **223**, pp. 289–343.

7. T. Mezger (2011). "The rheology handbook", Hanover, pp. 135-212.

8. A. Saasen (2002). "Sag of Weight Materials in Oil Based Drilling Fluids", paper *IADC/SPE 77190*, IADC/SPE Asia Pacific Drilling Technology 2002, Jakarta, Indonesia.

9. R. P. Jachnik (1997). "Rheological Characterization of Oil Based Drilling Fluids Utilizing Parallel Plate Geometries", *Ann. Trans. Nord. Rheol. Soc*., vol **5**, pp 135-138.

10. C. Ernhorn, A. Saasen (1996). "Barite Sag in Drilling Fluids", *Ann. Trans. Nord. Rheol. Soc*., vol **4**, pp 66-68.

11. B. Herzhaft, L. Rousseau, L. Neau, M. Moan, F. Bossard (2002). “Influence of temperature and clays/emulsion microstructure on oil-based mud low shear rate rheology”, paper *SPE 86197*, SPE Annual Technical Conference and Exhibition 2002, San Antonio, USA.

12. J. D. Ytrehus, A. Taghipour, S. Sayindla, B. Lund, B. Werner, A. Saasen (2015). "Full Scale Flow Loop Experiments of Hole Cleaning Performances of Drilling Fluids", paper *OMAE2015-41901,* submitted to OMAE 2015, St. John's, Canada.